1

Top quark working group report

Conveners: K. Agashe, R. Erbacher, C. E. Gerber, K. Melnikov, R. Schwienhorst

Contacts: M. Vos, A. Mitov, S. Wimpenny (top quark mass); M. Baumgart, A. Loginov, A. Garcia-Bellido, J. Adelman (top quark couplings); M. Schulze, A. Jung, J. Shelton (kinematics of top quark events); N. Craig, M. Velasco (rare decays of top quark); T. Golling, M. Perelstein, A. Ivanov, J. Hubisz (new particles decaying to/coupled to top-like final states); S. Chekanov, B. Tweedie, J. Pilot, R. Poeschl, J. Dolen (Top algorithms and detectors).

Contributors: S. Alioli, B. Alvarez-Gonzalez, D. Amidei, T. Andeen, A. Arce, B. Auerbach, A. Avetisyan, M. Backovic, Y. Bai, M. Begel, C. Bernard, C. Bernius, S. Bhattacharya, S. Birge, K. Black, A. Blondel, K. Bloom, T. Bose, J. Boudreau, J. Brau, G. Brooijmans, E. Brost, R. Calkins, D. Chakraborty, T. Childress, G. Choudalakis, V. Coco, C. Degrande, A. Delannoy, F. Deliot, L. Dell'Asta, E. Drueke, B. Dutta, A. Effron, K. Ellis, J. Erdmann, J. Evans, C. Feng, E. Feng, A. Ferroglia, K. Finelli, I. Fleck, A. Freitas, F. Garberson, R. Gonzalez Suarez, M. Graesser, N. Graf, Z. Greenwood, C. Group, A. Gurrola, G. Hammad, T. Han, Z. Han, U. Heintz, S. Hoeche, T. Horiguchi, A. Ismail, P. Janot, W. Johns, J. Joshi, A. Juste, T. Kamon, C. Kao, Y. Kats, A. Katz, M. Kaur, R. Kehoe, W. Keung, S. Khalil, A. Khanov, N. Kidonakis, C. Kilic, N. Kolev, A. Kotwal, J. Kraus, D. Krohn, M. Kruse, S. Lee, E. Luiggi, S. Mantry, A. Melo, D. Miller, G. Moortgat-Pick, M. Narain, N. Odell, Y. Oksuzian, M. Oreglia, A. Penin, Y. Peters, C. Pollard, J. Proudfoot, S. Rappoccio, S. Redford, M. Reece, F. Rizatdinova, R. Ruiz, M. Saleem, B. Schoenrock, C. Schwanenberger, E. Shabalina, P. Sheldon, F. Simon, K. Sinha, P. Skands, P. Skubik, G. Sterman, D. Stolarski, J. Stupak, S. Su, S. Thomas, E. Thompson, P. Tipton, E. Varnes, N. Vignaroli, D. Walker, K. Wang, B. Webber, S. Westhoff, D. Whiteson, M. Williams, S. Wu, U. Yang, H. Yohoya, H. Yoo, H. Zhang, N. Zhou, H. Zhu, J. Zupan.

1.1 Introduction

The top quark was discovered in 1995 [1, 2]; it is the heaviest elementary particle known today. Thanks to its large mass and the related strangth of its coupling to the Higgs boson, the top quark is often considered a key player in understanding the details of electroweak symmetry breaking. Studies of the top quark properties at the Tevatron and the run I of the LHC have given us a detailed understanding of many properties of this particle including its mass, its production and decay mechanisms, its electric charge and more. With the exception of the large forward-backward asymmetry in $t\bar{t}$ events observed at the Tevatron, all results on top quark pair and single top production obtained so far are consistent with the Standard Model.

Exploration of top quarks will be an integral part of particle physics studies at any future facility. In this report we describe what can be achieved with such studies. The report is organized along six topics:

- measurement of the top quark mass;
- studies of kinematic distributions of top-like final states;
- measuremnts of top quark couplings;

- searches for rare decays of top quarks;
- probing physics beyond the Standard Model with top quarks;
- algorithms for top quark identification at future facilities.

Main conclusions for each topic are presented in Sect.1.8

1.2 The top quark mass

The top quark mass is a parameter whose precise value is essential for testing the overal consistency of the Standard Model and the possible way it is embedded into various models of New Physics. The exact value of the top quark mass is also rucial for understanding if the Standard Model *without further extensions* can be continued to energies compared to the Planck scale, without running into problems with the stability of electroweak vacuum [3]. To put both of these statements into a perspective, we note that from precision electroweak fits, the 600 MeV uncertainty in the top quark mass corresponds to 5 MeV uncertainty in the W-mass (see e.g. Ref. [4]). Since the W-mass will be measured with this precision at future facilities, but signficant improvements in δM_W are not likely, we conclude that the future of the precision electroweak physics requires that the top quark mass is measured with the precision of about 0.5 GeV. On the other hand, the vacuum stability issue depends strongly on the value of the top quark mass. Indeed, as shown in Ref. [3], changing m_t by 2.1 GeV around the central value $m_t = 173.1$ GeV, the RGE scale where the Higgs quartic coupling becomes negative changes by *six* orders of magnitude, from $\mu_{\rm neg} \sim 10^8$ GeV to $\mu_{\rm neg} \sim 10^{14}$ GeV! It is easy to estimate that if m_t is known with 600 MeV uncertainty, as required by the electroweak fit, the scale can be estimated much more precisely, $\mu_{\rm neg} \sim (4.8 \pm 1.2) \times 10^{13}$ GeV. We conclude that the knowledge of the top quark mass with the $\mathcal{O}(0.5)$ GeV uncertainty will have an important impact on our understanding of particle physics while anything beyond that precision is an added bonus whose immediate applications are not obvious.

We note that a precision beyond 0.5 GeV in m_t can be easily reached at a lepton collider (ILC, CLIC, TLEP) through either the $t\bar{t}$ threshold scan or by direct reconstruction of the invariant mass distribution of top quarks when the collider is run at a higher energies. In both of these cases detailed simulations [5, 6] and advanceed theoretical computations (see e.g. Ref. [7] and references therein) show that the error on the top quark mass will not exceed $\mathcal{O}(100)$ MeV. We note that with respect of m_t determination, all lepton colliders that were suggested so far perform similarly[1] and that an additional attraction in measuring m_t at a lepton collider consists in a clean theoretical interpretation of the result of the measurement. As we explain below, the situation is different (more confusing) at a hadron collider although new methods for m_t measurements developed at the LHC help to mitigate this difference.

The value of the top quark mass, as quoted by the Particle Data Group, is $m_t = 173.5 \pm 0.6 \pm 0.8$ GeV. The total uncertainty on m_t is therefore close to 1 GeV; this is the highest relative precision available for *any* of the quark masses but it is a factor of two larger than the target precicion of 0.5 GeV motivated by the future of precision electroweak fits. It is an interesting question if m_t measurement with such a precision can be accomplished at the LHC. To answer it, we will first make some general remarks about measurements of m_t.

Existing measurements of the top quark mass rely on complex techniques that are caused by difficult hadron collider environment; the highest accuracy is currently reached using the so-called matrix-element method.

[1] We note that some improvements in m_t determination can be expected thanks to reduced breamstrahlubg at the muon collider and to the reduced beamstrahlung at TLEP.

We will explain a generic measurement of the top quark mass by considering the following example. Any measurment of the top quark mass is based on fitting a particular piece of data to a theory prediction where m_t enters as a free parameter. Hence, we write

$$D = T(m_t, \alpha_s, \Lambda_{\rm QCD}) = T^{(0)}(m_t) + \frac{\alpha_s}{\pi} T^{(1)}(m_t) + \mathcal{O}(\Lambda_{\rm QCD}/m_t), \tag{1.1}$$

where D on the left hand side is a particular kinematic distribution and T on the right-hand side is a theoretical prediction. We have indicated in Eq.(1.2) that the selected distribution should not be affected by non-perturabtive corrections; we will return to this point below. We also note that inclusion of QCD corrections necessitates a clear definition of the renormalization scheme which then fixes the mass parameter extracted from the fit. Since the two popular choices of the renormalized mass parameter – the pole mass and the $\overline{\rm MS}$ mass differ by almost 7 GeV, the specification of the renormalization scheme in the extraction of the top quark mass is an important issue. Solving Eq.(1.1), we find the top quark mass m_t. In general, the quality of such solution depends on the *accuracy* of the theoretical prediction that we have in the right hand side which is controlled by the order in perturbation theory included there. It is well-known that *majority* of the analyses are performed with leading order theoretical tool. In general, this amounts to setting $T^{(1)} \to 0$ in the above equation. The expected error on m_t is then

$$\delta m_t \sim \frac{\alpha_s}{\pi} \frac{T^{(1)}}{T^{(0)'}} \sim \frac{\alpha_s m_t}{\pi} \frac{T^{(1)}}{T^{(0)}} \sim \frac{\alpha_s}{\pi} m_t \sim 6 \text{ GeV}, \tag{1.2}$$

where $T^{(0)'} = {\rm d}T^{(0)}/{\rm d}m_t$ and we used $T^{(0)'} \approx T^{(0)}/m_t$. It is obvious from Eq.(1.2) that the estimated error in Eq.(1.2) is *significantly larger* than the current $\mathcal{O}(1)$ GeV error on m_t. We conclude that if m_t is obtained from a generic distribution at leading order, one can not, in general, expect the accuracy that is better than few GeV. Fortunately, there are two ways to get around this problem. The first one requires inclusion of NLO QCD corrections into a theory prediction; effectively, this pushes the error to $m_t(\alpha_s/\pi)^2 \sim 300$ MeV which is acceptable. The second one amounts to finding a kinematic distribution which has a *strong* dependence on m_t; in this case, ${\rm d}T^{(0)}/{\rm d}m \gg T^{(0)}/m_t$ and the estimate in Eq.(1.2) receives an additional suppression.

As we show below, *new* experimental techniques that address the question of the top quark mass determination roughly follow the two approaches described above. Incidentally, the above discussion can be used to argue that *well-established* methods for the top quark mass determination may have additional systematic errors which are not accounted for in their error budgets. Indeed, the matrix element method[2] is designed to maximize probabilities for kinematics of observed events by adjusting values of the top quark mass on an event-by=-event basis; it can be thought therefore as an attempt to fit a very large number of kinematic distributions for the best value of m_t.

An unsatisfacory feature of this methods is its "black-box" nature that does not allow one to understand which kinematic features of the top quark pair production process drive this sensitivity. While such methods – by design – should find distributions that show strong dependence on m_t, it is not clear if the relevant distributions are sensitive to non-perturbative effects whose description from first principles is not possible. Moreover, such approaches routinely rely on the use of parton shower event generators instead of proper QCD theory. This means that Eq.(1.1) becomes

$$D = T(m_t, \alpha_s, \Lambda_{\rm QCD}) \approx T^{(0)}_{\rm MC}(m_t, \alpha_s, \Lambda_{\rm QCD}, \text{tunes}), \tag{1.3}$$

where, as indicated in the last step, additional approximations, including parton shower tunes, are performed on the "theory" side. While the quality of this approximation *for the purpose of the top quark mass measurement* may be good, it is simply not clear how to assign the error to the parameter m_t which is extracted following this procedure. To make this problem explicit, the top quark mass extracted from Eq.(1.3) should be properly refered to as the "Monte-Carlo mass ", whose relation to m_t that enters the fundamental Standard Model Lagrangian is not understood.

[2]The template method is subject to similar arguments.

	Ref.[8]	Projections				
CM Energy	7 TeV	14 TeV				
Luminosity	$5fb^{-1}$	$100fb^{-1}$		$300fb^{-1}$		$3000fb^{-1}$
Pileup	9.3	19	30	19	30	95
Syst. (GeV)	0.95	0.7	0.7	0.6	0.6	0.6
Stat. (GeV)	0.43	0.04	0.04	0.03	0.03	0.01
Total, GeV	**1.04**	**0.7**	**0.7**	**0.6**	**0.6**	**0.6**

Table 1-1. *Expected precision of the top quark mass measurements that can be expected using conventional (likelihood-type) methods. Extrapolations are based on the published CMS lepton-plus-jets analysis. An additional* 300 MeV *systematic error is added to all extrapolated results.*

In spite of the caveats in the top quark mass determination that are inherent to conventional methods, it is interesting to estimate precision in m_t that can be achieved at the LHC. We do that using extrapolations of what has been accomplished at the Tevatron and during the run I of the LHC. In Table 1-1 we show such projections for conventional methods assuming that the mass is measured in the lepton + jet channel for the 14 Tev LHC for different integrated luminosities and pile-up scenarios. We assume the $t\bar{t}$ production cross-section to be $\sigma_{pp\to t\bar{t}} = 167(951)$ pb at 7 and 14 TeV LHC, respectively. It follows from Table 1-1 that conventional methods may, eventually, lead to the measurement of the top quark mass with an error of about 0.6 GeV and that this error is totally dominated by systematic uncertainties. It is interesting to point out that precision in m_t saturates for the integrated luminosity of 300 fb^{-1} and that there is no benefit of using yet higher luminosity for the top quark mass measurement. The reason for this is the increased pile-up and related degradation of the jet energy scale determination in the high-luminosity environment. Note, however, that the systematic error estimate in Table 1-1 includes 300 MeV that is added to all extrpolated results to account for unforseen sources of systematics; without these 300 MeV uncertainties, the error on the top quark mass measurement becomes very small.

Conceptual problems with conventional methods can be mitigated be measuring the top quark mass from well-defined kinematic distributions which, on one hand, are sufficiently senstitive to m_t and, on the other hand, can be cleanly interpreted in terms of a particular type of the top quark mass. The latter requirement forces us to select kinematic distributions that are infra-red safe, so that their computations in higher-orders of QCD perturbation theory can be performed. In addition, methods for measuring the top quark mass should, ideally, be immune to contaminations from beyond the Standard Model physics – a scenario that is concievable if there is top-like BSM physics at the energy scale close to $2m_t$. For example, if m_t is determined from the total cross-section $\sigma_{pp\to t\bar{t}}$ and if $pp \to t\bar{t}$ receives unknown contributions from top-like BSM physics, the extracted value of the top quark mass will be smaller than the true m_t. This scenario can occur for example in SUSY models with light stop squarks $m_{\tilde{t}} \sim m_t$ that are still experimentally viable.

Methods for top quark mass determination that are based on the analysis of kinematic distributions of top quark decay products are as close to an ideal method as possible. The main reason is that, up to small effects related to selection cuts and combinatorial backgrounds, such distributions are Lorentz invarint and therefore completely decouple the production stage from the decay stage. This minimizes impact of any physics related to $t\bar{t}$ production on the top quark mass measurement. We will describe two of the methods that belong to this category – the "end-point" method developed recently by the CMS collaboration [9] and the J/ψ method suggested long ago in Ref. [10].

	Ref.[9]	Projections		
CM Energy	7 TeV	14 TeV		
Luminosity	$5fb^{-1}$	$100fb^{-1}$	$300fb^{-1}$	$3000fb^{-1}$
Syst. (GeV)	1.8	1.0	0.7	0.5
Stat. (GeV)	0.90	0.10	0.05	0.02
Total	**2.0**	**1.0**	**0.7**	**0.5**

Table 1-2. *Projections for the uncertainty in m_t determined using the CMS end-point method [9]. Extrapolations are based on the published CMS analysis.*

The idea of the end-point method is based on the observation that the invariant mass distribution of a lepton and a b-jet contains a relatively sharp edge whose position is correlated with m_t. Therefore, by measuring the position of the end-point, one can determine the top quark mass. The number of events close to the end-point is fitted to a linear combination of a flat background and a linear function $N_{lb} \sim N_{\rm bck} + S(m_{\rm lb} - m_0)$; m_0 gives the position of the end-point. The attractive feature of this method is that it is (almost) independent of any assumption about the matrix element and that it clearly measures either the pole mass *or* some "kinematic" mass which is close to it. At the expense of being more (Standard) model-dependent, one can actually improve on this method by utilizing not *only* the position of the end-point but also the shape of the $m_{\rm lb}$ distribution. Note that away from the kinematic end-point the shape of m_{lb} distirbution is acurately predicted through NLO QCD including off-resonance contributions and signal-background interfernces [11, 12], while close to the end-point re-summed predictions are required that are not available at present.

Nevertheless, even without potential improvements, the end-point method offers an interesting alternative to conventional methods. Uncertainties in m_t that one may hope to achieve are estimated in Table 1-2. We note that by using the end-point method we *do gain in precision by going to high-luminosity LHC*. Our projections show that the error as small as 500 MeV can be reached. The dominant contribution to systematic uncertainty for each of these studies is the jet-energy scale and hadronization uncertainties. Similar to estimate of δm_t that can be achieved using conventional methods, we add 300 MeV to systematic uncertainty in Table 1-2, to account for unforseen sources of the systematics.

Another approach to measuring the top quark mass that is very different from conventional ones is the so-called J/ψ method. Here the top quark mass is obtained from the invariant mass distribution of three leptons from the *exclusive* decay of the top quark $t \to eB \to eJ/\psi \to eee$. The extrapolations for the J/ψ-method are shown in Table 1-3. The attractive feature of this approach is its absolute complimentarity to more traditional methods discussed above. The uncertainties in case of the J/ψ method are dominated by statistical uncertainties for luminosities below 100 fb^{-1} and by theory uncertainties for higher luminosities. The theory uncertainties in m_t are estimated to be of the order of 1 GeV; they are caused by scale and parton distribution functions uncertainties and by uncertainties in $b \to B$ fragmentation function. Some reduction of theory uncertainties can be expected although dramatic improvements in our knowledge of the fragmentation function are not very likely. This is reflected in the change of the theory error shown in Table 1-3 for 14 TeV LHC with 3000 fb^{-1} where it is assumed that NNLO QCD computation of the exclusive production of J/ψ in $t\bar{t}$ events will become available and that the scale uncertainty will be reduced by a factor of two.

We note that other methods of measuring m_t with relatively high precision are possible and were, in fact, discussed in the literature. On the experimental side, the three-dimensional template fit method was recently presented by the ATLAS collaboration [13]. The key idea here is to determine the top quark mass, the light-

	Ref. analysis	Projections				
CM Energy	8 TeV	14 TeV			33 TeV	100 TeV
Luminosity	$20fb^{-1}$	$100fb^{-1}$	$300fb^{-1}$	$3000fb^{-1}$	$3000fb^{-1}$	$3000fb^{-1}$
Theory (GeV)	-	1.5	1.5	1.0	1.0	0.6
Stat. (GeV)	7.00	1.8	1.0	0.3	0.1	0.1
Total	**-**	**2.3**	**1.8**	**1.1**	**1.0**	**0.6**

Table 1-3. *Extrapolations of uncertainties in top quark mass measurements that can be obtained with the J/Ψ method.*

quark jet energy scale and the b-quark jet energy scale from a simultaneous fit to data, thereby transforming a large part of the systematic uncertainty related to jet energy sclaes to a statistical one. The error of this measurement is not competitive with other m_t-determinations at the moment, but the key idea of the method can be applied in conjunction with other methods and will, hopefully, help to reduce systematic uncertainties. Another potentially interesting opportunity is provided by the top quark mass measurements based on exploiting m_t-dependence of lepton kinematic distributions. Although such studies were not actively pursued experimentally, they may offer an interesting avenue for the top quark mass measurement in the high-pile-up scenario given their independence of jet energy scale uncertainties. Theoretical studies of some lepton distirbutions and their sensitivity to m_t were performed through NLO QCD in Ref. [14] with the conclusion that $\mathcal{O}(1.5)$ GeV error on m_t can be achived, but further studies that include more realistic estimates of uncertainties are clearly warranted. Finally, it was proposed recently to employ $t\bar{t}j$ events to constrain the top quark mass [15]. This method is clean theoretically and appears to be feasibly experimentally; as shown in Ref. [15], the $\mathcal{O}(1)$ GeV uncertainty in m_t can be achieved.

We conclude by making a general remark about the future of the top quark measurements at a hadron collider. While hadron collider measurements of the top quark mass *can not* compete with e^+e^- colliders, our discussion shows that it is possible to have a number of top quark measurements at the LHC, including the high-luminosity option, which are both theoretically clean and show high sensitivity to m_t. It is also important to stress that these measurements are limited by different types of uncertainties, so that combining their results assuming that errors are uncorrelated is a reasonable thing to do. A combination of the results of different measurements can lead to further reduction in the error on m_t that is achievable at the LHC, pushing it to a $0.3 - 0.4$ GeV range.

1.3 Top quark couplings

The coupling of the top quark to the W and Z bosons, the photon and the gluon, and the Higgs boson are explored in this section. The couplings are measured in top quark production as well as in the top quark decay. This section compares the low-and high-luminosity LHC to the ILC. Higher-energy hadron colliders are not expected to improve the measurements beyond the LHC sensitivity and are thus not studied here. The muon collider similarly allows for the same studies as done at the ILC, but with smaller beam-related uncertainties and higher luminosity. TLep provides larger data samples than the ILC but has insufficient energy to measure the top Yukawa coupling. The top quark couplings sensitivity is compared here using the coupling notation, a full description is in terms of effective operators [16, 17].

1.3.1 Strong interaction

The strong interaction of the top quark is measured in top quark pair production at hadron colliders. The cross section has been measured at the Tevatron and at the LHC. The strong coupling of the top quark is also studied in top quark pair events together with additional jets.

The theoretical prediction for the top pair production cross section at hadron colliders has been computed at NNLO in the strong coupling. The scale uncertainty is 3.5%, of the same order of magnitude as the experimental uncertainties at the 8 TeV LHC. The LHC cross section measurements are not expected to improve beyond the current 5% level of uncertainty, the focus instead is on differential cross sections (see Section 1.4.

Four-fermion operators in the strong interaction have also been explored. These are accessible only at the LHC. Limits on the scale probed in the $u\bar{u}t\bar{t}$ four-fermion coupling at the 3000 fb^{-1} range from a conservative estimate of 1.2 TeV to a optimistic estimate of 3 TeV [18].

The top pair production cross section at a lepton collider depends on the strong coupling through higher order corrections. The top mass threshold scan described in Section 1.2 yields not only a top mass measurement but also a precise determination of the strong coupling constant α_s. The expected statistical precision on α_s is better than 0.1% [6].

1.3.2 Weak interaction: W boson

The coupling of the top quark to the W boson is studied in top quark decays and in single top quark production at the LHC and the Tevatron, and in top quark decays at the linear collider. The effective Lagrangian describing the Wtb interaction including operators up to dimension five is [16]:

$$\begin{aligned}\mathcal{L} = & -\frac{g}{\sqrt{2}}\bar{b}\gamma^{\mu}(V_L P_L + V_R P_R)tW^-_{\mu} \\ & - \frac{g}{\sqrt{2}}\bar{b}\frac{i\sigma^{\mu\nu}q_{\nu}}{M_W}(g_L P_L + g_R P_R)tW^-_{\mu} + h.c.\,, \end{aligned} \tag{1.4}$$

where M_W is the mass of the W boson, q_ν is its four-momentum, $V_L = V_{tb}$ is the left-handed coupling, which in the SM is equal to the Cabibbo-Kobayashi-Maskawa matrix element [19], and $P_L = (1-\gamma_5)/2$ ($P_R = (1+\gamma_5)/2$) is the left-handed (right-handed) projection operator. The right-handed vector coupling V_R and the left-and right-handed tensor couplings g_L and g_R are zero in the SM.

The measurement of the helicity of the W boson in top quark decays can distinguish SM-like left-handed vector couplings from right-handed vector and from left-or right-handed tensor couplings. This measurement of the angular correlations in the tWb vertex provides information about ratios of couplings. The current reach for the anomalous couplings with 8 TeV data is of the order of 10^{-1}.

Single top quark production involves the tWb vertex in top quark production and thus also provides information on the magnitude of the tWb coupling and the CKM matrix element $|V_{tb}|$. Single top quarks are produced in three different modes, t-channel with the largest cross section, Wt associated production with the next-largest cross section, and s-channel which has a very small cross section. The three modes have different sensitivities to new physics and anomalous couplings. LHC measurements of single top quark production, in particular in the t-channel mode are also sensitive to off-diagonal CKM matrix elements [20]. The single top production cross section measurement is dominated by systematic uncertainties already in the current

dataset [21, 22, 23], and the situation is not expected to improve much at higher energies or with larger datasets. The ultimate cross section uncertainty will likely be around 5%, similar to top pair production, meaning the coupling and $|V_{tb}|$ uncertainty will be around 2.5%. Searches for anomalous couplings in the tWb vertex depend on the ability to separate the signal from backgrounds are are less limited by systematic uncertainties. A search for CP violation through an anomalous coupling gives a limit on $Im(g_R)$ [24]. An extrapolation of the sensitivity to anomalous couplings from single top quark production and decay gives an expectation of about 10^{-2} for the anomalous coupling sensitivity with 300 fb^{-1}.

The tWb coupling can also be probed at a γe collider, with a reach of 10^{-1} to 10^{-2} [25]. Similarly, an electron-proton collider of sufficient energy to produce single anti-top quarks is also sensitive to anomalous tWb couplings. The reach is about 10^{-3} to 10^{-2} for a LHC-based electron-proton collider with a CM energy of 1.3 TeV [26].

The width of the top quark can be determined indirectly at the LHC through t-channel single top quark production. The width of the top quark is determined with high precision at the ILC in the threshold scan. The tWb coupling can also be probed indirectly at a lepton collider through a scan at CM energies between m_t and $2m_t$.

1.3.3 Electroweak interaction: Z boson and photon

The interaction of the top quark with the Z boson and the photon has not been measured yet. This coupling is being probed at the LHC in a challenging measurement. It will be measured with high precision at lepton colliders. The constraints on the coupling of the top quark to the photon and Z boson use the expression [27]

$$\Gamma_{\mu}^{ttX} = ie\left\{-\gamma_m u\left((F_{1V}^X + F_{2V}^X) + \gamma_5 F_{1A}^X\right) + \frac{(q-\overline{q})_\mu}{2m_t}\left(F_{2V}^X - i\gamma_5 F_{2A}^X\right)\right\},$$

where X is either a photon ($X = \gamma$) or Z boson ($X = Z$). The SM couplings are F_{1V}^{γ}, F_{1V}^{Z} and F_{1A}^{Z}.

The LHC experiments have measured the production of photons in association with top quark pairs, and will measure both the $\gamma + t\bar{t}$ and $Z + t\bar{t}$ cross sections. However, the Feynman diagrams for both processes mainly involve not only the $t\gamma$ coupling of interest, but also emission of a γ or Z boson from the final state products. There is also emission of photons from initial state quarks, however the $q\overline{q}$ initial state contributes only a small cross section at the LHC. Extracting the top-photon or top-Z coupling from the associated production measurements leads to uncertainties in the coupling measurements and relies on a detailed theoretical understanding of the production process [27].

Single top quark production in association with a Z boson can also be used to study the tZ coupling, it provides additional information and involves both the tZ and WZ couplings.

The ultimate precision in the $t\gamma$ and tZ couplings will come from the linear collider where these couplings can be measured with high precision [28]. However, the two couplings are entangled in the top pair production process and theory input as well as model assumptions are required to separate them. For the projections in Tab. 1-4, electron and positron polarizations of 80% and 30%, respectively, are assumed.

Most of the top quark couplings to the photon and the Z boson can be measured at the ILC to a precision that is typically an order of magnitude better than at the LHC. The precision accessible at TLep should be somewhat better than that at the linear collider due to the higher integrated luminosity. A muon collider provides larger integrated luminosity and smaller beam uncertainties, but also challenging backgrounds, thus it is not clear if it will be able to improve on the ILC measurements.

Collider	LHC		ILC
CM Energy [TeV]	14	14	0.5
Luminosity [fb^{-1}]	300	3000	500
SM couplings			
photon, F_{1V}^{γ}	0.042	0.014	0.002
Z boson, F_{1V}^{Z}	0.50	0.17	0.003
Z boson, F_{1A}^{Z}	0.058	0.17	0.005
Non-SM couplings			
photon, F_{2V}^{γ}	0.037	0.025	0.003
photon, F_{2A}^{γ}	0.017	0.011	0.007
Z boson, F_{2V}^{Z}	0.25	0.17	0.006
Z boson, ReF_{2A}^{Z}	0.35	0.25	0.008
Z boson, ImF_{2A}^{Z}	0.035	0.025	0.015

Table 1-4. *Expected precision of the top quark coupling measurements to the photon and the Z boson at the LHC [18] and the linear collider [28].*

1.3.4 Yukawa coupling

The coupling of the top quark to the Higgs boson is being measured at the LHC in many final states. It will also be studied in detail at lepton colliders. More details on the top Yukawa coupling measurements can be found in the Higgs working group report.

The cross section for $t\bar{t}H$ is small at the LHC and has many final states, depending on the top quark decay mode (lepton+jets or di-lepton) and the Higgs decay mode ($b\bar{b}$ or $\gamma\gamma$ or WW or others). Each final state has a its own unique, typically large background, mainly from top quark pair production in association with jets or bosons. The coupling of the top quark to the Higgs boson is extracted from these measurements with relatively large uncertainties of about twenty percent initially, with an improvement to ten percent percent at the high-luminosity LHC [29, 30]. The $t\bar{t}H$ final state with the highest luminosity is also a promising channel to measure the muon coupling of the Higgs boson.

Better precision in the top-Higgs coupling is expected from lepton colliders running at a sufficiently high CM energy and collecting a large integrated luminosity. Initial studies focused on a CM energy of 800 GeV where the $t\bar{t}H$ cross section is largest, however a measurement at 500 GeV is also possible. For the projections in Tab. 1-5, electron and positron polarizations of 80% and 30%, respectively, are assumed. For the ILC, a luminosity of twice the design luminosity is assumed. A comparison of the Top Yukawa coupling precision expected at different colliders is shown in Tab. 1-5. It is not possible to measure the top Yukawa coupling at TLep due to the insufficient CM energy.

1.4 Kinematics of top-like final states

Working with top quarks clearly requires us to understand how they are produced and how they decay. In this Section, we explore what we know about this and what can be expected given the current knowledge

Collider	LHC		ILC	CLIC
CM Energy [TeV]	14	14	0.5	800
Luminosity [fb^{-1}]	300	3000	1000	1000
Top Yukawa coupling κ_t	$(20-25)\%$	$(8-20)\%$	10%	6%

Table 1-5. *Expected precision of the top quark Yukawa coupling measurement expected at the LHC and the linear collider [28]. The range for the LHC precision corresponds to an optimistic scenario where systematic uncertainties are scaled by 1/2 and a conservative scenario where systematic uncertainties remain at the 2013 level [29, 30]. The ILC [28] and CLIC [31] projections assume polarized beams and large integrated luminosities.*

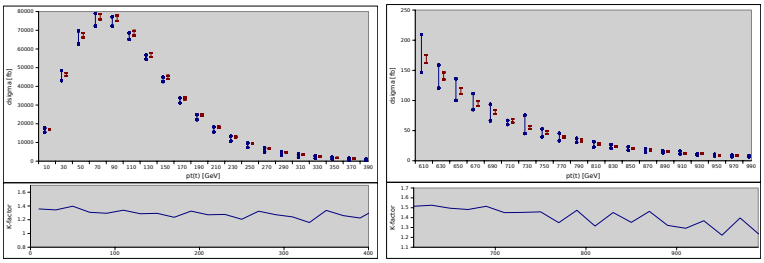

Figure 1-1. *NLO QCD predictions [33] for transverse momentum, rapidity and rapidity difference at the 14 TeV LHC. Blue error bars correspond to scale variation by a factor of two around $\mu = m_t$. Dark red error bands correspond to variation of different MSTW pdf error sets.*

and expected improvements in the future. While such discussion is interesting in its own right, it also allows us to understand to what extent *deviations* from expected behavior of various top quark distributions in various regimes can be probed at existing and future facilities. This summary is based on the summary White Paper submitted to Snowmass 2013 by the Top Kinematics working group [32].

1.4.1 Theoretical Predictions

Our current understanding of top quark pair production in hadron collisions is based on next-to-leading order computations for fully-differential process $pp \to t\bar{t} \to W^+W^-b\bar{b}$ both within and beyond the narrow width approximation. Such computations are also extended to higher-multiplicity processes by either theoretical results for $t\bar{t}+j$ and also matched to parton showers. Existing theoretical results will be further improved by by extending available results for differential quantities to next-to-next-to-leading order in perturbative QCD; such results for the total cross-section $pp \to t\bar{t}$ were recently obtained.

We will now take a closer look at the quality of theoretical description of various kinematic distributions. To this end, we show $p_\perp, y_t$ and $|y_t - y_{\bar{t}}|$ in $pp \to t\bar{t}$ at the 14 TeV LHC and indicate the uncertainties in the predictions caused by imperfect knowledge of parton distribution functions and missing higher-order corrections that we estimate by varying renormalization and factorization scales by a factor of two. We see that scale uncertainties dominate and that the error on theory predictions is are at the level of twenty percent.

Another interesting kinematic region is the boosted one and, as we will show in a second, it is more difficult to understand the uncertainty in the theoretical prediction for this quantity. Indeed, a straighforward MCFM

computation shows that for $p_\perp > 800$ GeV, the uncertainty on rapidity and $p_\perp$ distributions roughly double compared to the non-boosted regime. On the other hand, we note that computations that are based on both soft resummation and SCET point towards additional *positive* contirbutions to $p_\perp$ distributions at high value of top quark momentum. One can speculate that – being positive – this effect may be caused by a high-probability of the process where a top quark produced in association with two jets. If true, it should be possible to obtain the correct shape of $p_\perp$ disrtibuion by considering samples of $t\bar{t}$, $t\bar{t}+j$ and $t\bar{t}+2j$ etc. matched along the lines of the CKKW/MLM framework. Whatever the true reason for this increase, it will be interesting to see if forthcoming NNLO computations for this region will also indicate a signficant positive contribution to $p_\perp$-distribution.

1.4.2 Top Quark Pair Forward-Backward asymmetry

Quantum chromodynamics predicts that $t\bar{t}$ production in quark and antiquark collisions is forward-backward symmetric at leading order. However, the SM predicts a small positive asymmetry at higher orders [34, 35, 36], such that the top quark is preferentially emitted in the direction of the incoming quark, while the anti-top quark follows the direction of the incoming antiquark. Several beyond the standard model (BSM) production mechanisms that exchange new bosons could enhance the forward-backward asymmetry, so deviations from the SM prediction could represent a glimpse to new physics.

The Tevatron has the advantage that $q\bar{q}$ annihilation dominates the $t\bar{t}$ production, while there is no asymmetry in the gluon fusion $t\bar{t}$ production that dominates at the LHC. Inclusive asymmetries measured at the Tevatron exceed SM predictions by almost 3 SD [37, 38], with larger mass and rapidity dependence than predicted by the SM. The asymmetry in one particular subset of CDF data differs by more than three SD from the NLO prediction. At the LHC, the ATLAS and CMS Collaborations have performed measurements of the difference in angular distributions between top quarks and antiquarks using asymmetries based on the $t\bar{t}$ rapidities (A_{FC}) [39, 40], which agree with SM predictions. Here we detail some estimates toward the measurability of the SM forward-backward asymmetry A_{FC} at the 14 TeV LHC, as well as introducing new observables that may be used in the analyses.

The increased center of mass energy, relative to LHC 7 and LHC 8, increases the proportion of $t\bar{t}$ events that arise from (symmetric) gluon fusion, so the size of the signal decreases with increasing center of mass energy. Already at LHC 7, measurements of the top forward-central asymmetry are systematically limited. SM predictions for LHC 14 as a function of cuts on minimum top pair invariant mass $m_{t\bar{t}}$ or velocity $\beta_{t\bar{t}}$ are calculated in Ref. [41]. Specifically, we use predictions for the quantity

$$A_{FC}^{\eta} = \frac{N(\Delta|\eta| > 0) - N(\Delta|\eta| < 0)}{N(\Delta|\eta| > 0) + N(\Delta|\eta| < 0)} \tag{1.5}$$

where $\Delta|\eta| \equiv |\eta_t| - |\eta_{\bar{t}}|$ looks at whether the reconstructed top or anti-top is more central according to lab-frame *pseudo-rapidity*. Cutting on either CM invariant mass or CM rapidity increases the proportion of q-$\bar{q}$-initiated top pair events relative to gluon-initiated events, and thus enhances the signal. However, even with kinematic cuts, the size of the signal at the 14 TeV LHC is comparable to the systematic uncertainties on the current measurements. The dominant contributions to the systematic errors identified by the collaborations are: jet energy scale, lepton identification, background modeling ($t\bar{t}$, $W+$ jets, multijets), and model dependence of signal generation and the unfolding procedure. Several of these can certainly improve with luminosity, in particular jet energy scale and lepton identification. Possible improvements in background modeling are less clear.

In Fig. 1.4.2 we plot both statistical and combined statistical+systematic uncertainties for three different scenarios regarding the evolution of the systematic uncertainties with luminosity. Statistical errors are

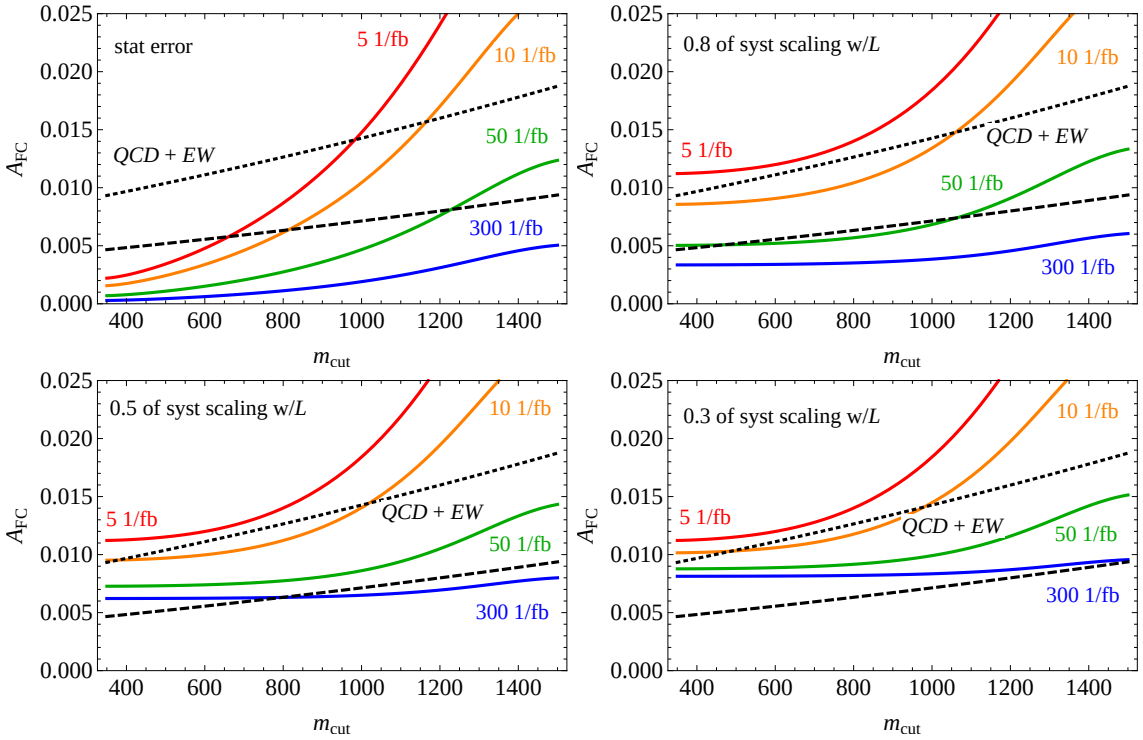

Figure 1-2. *SM asymmetry compared to projected uncertainty on the measurement in the lepton+jet channel at LHC 14, as a function of minimum $m_{t\bar{t}}$, with three different scenarios for the improvement of systematic uncertainties with luminosity. The dotted line shows the SM (QCD and EW combined) predictions of Ref. [41], and the dashed line shows 0.5 × the asymmetry to indicate 95% CL sensitivity. Top left: statistical error only. Top right: statistical error combined in quadrature with systematic error at 5 fb^{-1}, with 0.8 of the systematic uncertainty scaling as $1/\sqrt{\mathcal{L}}$. Bottom left: statistical error combined in quadrature with systematic error at 5 fb^{-1}, 0.5 of which scales as $1/\sqrt{\mathcal{L}}$. Bottom right: statistical error combined in quadrature with systematic error at 5 fb^{-1}, 0.3 of which scales as $1/\sqrt{\mathcal{L}}$.*

shown assuming semi-leptonic top pair decays with an approximate (flat) efficiency for top identification and reconstruction of $\epsilon = 0.2$ per (semi-leptonic) event. This efficiency represents the requirement that at least one (isolated) lepton and at least 4 jets lie within $|\eta| < 2.4$, with $p_{T,j} > 30$ GeV, $p_{T,e} > 30$ GeV, and $p_{T,\mu} > 20$ GeV, with the further requirement that solving quadratic equations for the missing neutrino four-momentum yield a physical solution. The cross-section is normalized to a NLO prediction of 845 pb using a constant K-factor. In all cases we take the systematic uncertainty at 5 fb^{-1} to be given by the systematic uncertainty reported by CMS with 5 fb^{-1} of LHC 7 data, and then evolve the systematic uncertainties with luminosity assuming a fraction $(0.3, 0.5, 0.8)$ of the systematic uncertainty scales as $1/\sqrt{\mathcal{L}}$. Based on this estimate, with sufficient luminosity, LHC14 will have sensitivity to the SM asymmetry if at least 0.5 of the systematic errors scale with luminosity.

The dileptonic channel offers another window into top pair production asymmetries, albeit at smaller statistics due to the reduced branching fraction. Current LHC measurements in the dileptonic channel are done at 7 TeV and have, with 5 fb^{-1}, systematic uncertainties of 0.7%, comparable to those in the semileptonic channel [42, 43]. An alternate possibility in the dileptonic channel is to measure an asymmetry

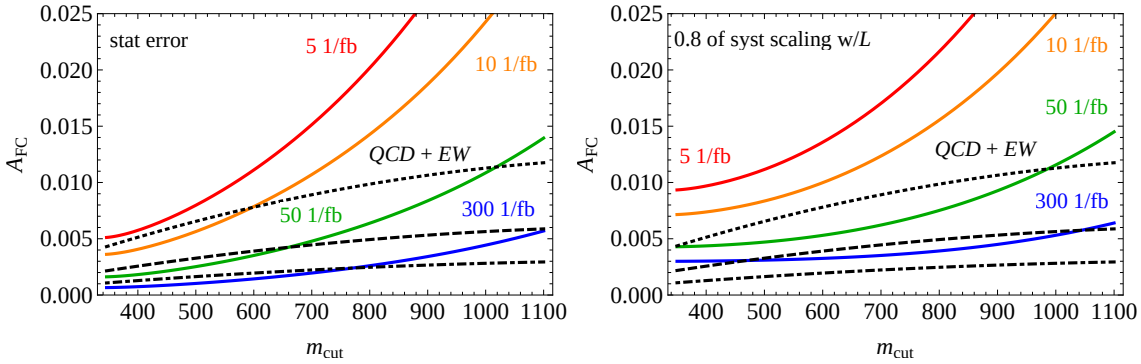

Figure 1-3. *SM* inclusive *lepton asymmetry compared to projected uncertainty on the measurement at LHC 14, as a function of minimum $m_{t\bar{t}}$, with and without systematic uncertainties. The dotted line shows the SM (QCD and EW combined) predictions of Ref. [44], the dashed line shows 0.5 × the asymmetry, and the dash-dotted line shows 0.25 the asymmetry to give a rough estimate of 95% CL sensitivity recalling the washout due to finite lepton acceptance cuts. Left: statistical error only. Right: statistical error combined in quadrature with systematic error given by $\Delta A = 0.007$ at 5 fb^{-1}, with 0.8 of the systematic uncertainty scaling as $1/\sqrt{\mathcal{L}}$.*

of the leptons rather than of the tops themselves,

$$A_{\ell\ell} = \frac{N(\Delta|\eta_\ell| > 0) - N(\Delta|\eta_\ell| < 0)}{N(\Delta|\eta_\ell| > 0) + N(\Delta|\eta_\ell| < 0)}, \tag{1.6}$$

where $\Delta|\eta_\ell| \equiv |\eta_{\ell^+}| - |\eta_{\ell^-}|$. The systematic uncertainty quoted in the measurement of this leptonic asymmetry is smaller than the uncertainty on the parent top asymmetry. However, the asymmetry itself is also smaller, especially when realistic geometric acceptance cuts are taken into account. To estimate the reach in the leptonic asymmetry we use an approximate (flat) efficiency for top pair identification and reconstruction of $\epsilon = 0.25$ per dileptonic top pair event, again accounting for geometric and p_T acceptance and an additional finite efficiency for reconstructing the top pair from the measured missing momentum. Results are shown in Fig. 1.4.2. Observation of the SM effect in this channel does not look promising; the reduction in the systematic error bars is more than compensated by the intrinsically smaller signal.

1.4.3 Benchmark Axigluons for the Tevatron anomaly

Out of the vast zoology of proposed BSM explanations for the Tevatron anomaly in the top forward-backward asymmetry, axigluons [45, 46, 47] are left looking most plausible after the low-energy LHC run has been completed. Table 1-6 shows a compilation of some benchmark axigluon models which can help explain the Tevatron anomaly without contradicting other searches as of July 2013. Detailed discussions of experimental constraints on axigluon models can be found in [48] for "light" ($M_{G'} < 450$ GeV) axigluons and in [49] for heavy axigluons. These benchmarks are phenomenological, insofar as they do not provide a UV-complete description of the axigluon sector, and would require additional model-building to construct a full theory [50, 47, 51]. However, they provide useful descriptions of the BSM state whose couplings are directly related to the Tevatron anomaly. In the absence of further reasons to prefer a specific BSM UV framework, this phenomenological approach is most economical for defining collider targets.

Model	mass (GeV)	Γ/m	g_q (g_s)	g_t (g_s)
Light A	250	0.2	0.35	0.35
Light B	400	0.2	0.4	0.4
Heavy A	2000	0.15	0.3	-3
Heavy B	2000	0.2	0.7	-1.5

Table 1-6. *Benchmark axigluon models for the Tevatron A_{FB} anomaly. Axial couplings to light quarks g_q and to top quarks g_t are given in units of the strong coupling constant. The broad widths of all benchmarks except "Heavy A" require the presence of additional BSM decay modes.*

1.4.4 New observables for A_{FB} at LHC

In contrast to A_{FC} in $t\bar{t}$ production the asymmetry in $t\bar{t}+j$ final states has the advantage that NLO calculations are available [52, 53]. A recent study documented in [54, 55] introduces two new observables in $t\bar{t}+j$ events. Two different planes are defined in these kind of events due to momentum conservation: one is given by the t, $\bar{t}$ and the additional jet and the other one by the incoming partons and the additional jet. Employing the inclination between these planes an *incline asymmetry* can be defined, which is of equal or larger size than the standard definition of A_{FC}. Furthermore another new observable is introduced using the energy of the t and the $\bar{t}$ quark, hence called *energy asymmetry*. Ref. [54] states that this is also sensitive to A_{FC} in the qg production channel.

In $t\bar{t}+j$ the incline asymmetry benefits from the additional information provided by the $t\bar{t}+j$ event kinematics. Ref. [54] finds that it is possible to measure an incline asymmetry of the order of 4% with a significance of three standard deviations with 100 fb^{-1} at 14 TeV. Extrapolating this to 3000 fb^{-1} of integrated luminosity yields about 16 s.d. for both observables. It should be mentioned that the calculations carried out for the new observables are currently at leading order and NLO corrections to the new observables could be sizable and affecting the projected sensitivities.

1.4.5 Asymmetry at LHCb

Measurement of a top rate asymmetry at the LHCb experiment could provide further information into top quark asymmetry [56]. A LHCb internal study is currently done, which investigates also other final states including dilepton final states. The aim of the study is to provide for all final states (and center-of-mass energy) the expected asymmetry and related uncertainties. Depending on the convergence the study could also include more detailled statements on systematic uncertainties. In terms of a cross section measurement at LHCb this study will state the expected yields per inverse fb in the acceptance of LHCb for different final states.

Expect to have results of this internal LHCb study on expected sensitivity of asymmetry measurements, which should be available publicly by end of July.

1.4.6 Top quark spin correlations

Top quark spin correlations are a unique tool for studying the interplay between electroweak and strong physics in the top quark sector. After the observation of top quark spin correlations at the Tevatron [57] and recently at the LHC [58, 59], experimental analyses will soon be able to probe the effects of New Physics models on SM spin correlations.

The cleanest $t\bar{t}$ samples are the ones with two opposite sign leptons in the final state. Spin correlations in this di-leptonic decay mode manifest them self most prominently in the angle between the two leptons. In fact, the azimuthal opening angle has been shown to be most robust under higher order corrections and parton showering effects. The effects of higher order corrections have been studied e.g. in Refs. [60, 61]. For standard acceptance cuts, NLO QCD effects introduce shape changes of at most 20 percent. If additional cuts are applied that enhance spin correlations, NLO corrections increase the correlation even further. Electroweak corrections have negligible effects and scale variations are vanishing small because distributions are typically normalized On the experimental side, the reconstruction of the lepton opening angle in the laboratory frame does not involve kinematics of other particles and can therefore be extracted with small systematic uncertainties. The normalized azimuthal opening angle distribution is therefore an ideal observable for studying top quark spin correlations. Of course, other constructions such as helicity angles, double differential distributions and asymmetries can also be explored.

It has been shown that top quark spin correlations can be used to distinguish SM top quarks from scalar or fermionic partners. In case of the discovery of a new resonances which decays into $t\bar{t}$ pairs, top quark spin correlations can also be used to analyze the couplings of this new particle [62, 63]. Another interesting aspect are New Physics contributions to the top quark chromomagnetic $\hat{\mu}_t$ and electric $\hat{d}_t$ dipole moments. Refs. [64, 65] demonstrate that New Physics contributions to $\hat{\mu}_t$ and $\hat{d}_t$ can be exposed through spin correlations in the di-leptonic and in the semi-leptonic decay mode. From the dileptonic sample of the 20 fb^{-1} run at 8 TeV, it should be possible to constrain Re$\hat{\mu}_t$ and Re$\hat{d}_t$ at the few percent level. The imaginary parts Im$\hat{\mu}_t$ and Im$\hat{d}_t$ can be constrained from lepton-top helicity angles in the semi-leptonic channel where a full reconstruction of the $t\bar{t}$ system is possible. Using the same dataset limits of about 15-20 percent are possible. Ref. [64] finds that constraints of 1 percent or below are possible with 100 fb^{-1} at 13 TeV.

1.5 Rare decays

1.5.1 Introduction

Extensions of the SM often induce new flavor-violating couplings between the top quark and other Standard Model particles, typically through new physics (NP) running in loops. In contrast, flavor-changing neutral couplings of the top are highly suppressed in the SM, so that the measurement of anomalous or flavor-violating couplings of the top quark provides a sensitive probe of physics beyond the Standard Model. As the top quark decays before hadronizing, top flavor violation is ideally probed through direct flavor-changing neutral current (FCNC) production and decays of the top quark in experiments at the energy frontier.

Although flavor-violating couplings of the top may arise from many sources, if the responsible NP is heavier than the top, it can be integrated out and its effects described by an effective Lagrangian: for details, see, for example, [66].

Table 1-7. *SM and NP predictions for branching ratios of top FCNC decays. The SM predictions are taken from [67], on 2HDM with flavor violating Yukawas [67, 68] (2HDM (FV) column), the 2HDM flavor conserving (FC) case from [69], the MSSM with 1TeV squarks and gluinos from [70], the MSSM for the R-parity violating case from [71, 72], and warped extra dimensions (RS) from [73, 74] .*

Process	SM [67]	2HDM(FV) [67, 68]	2HDM(FC) [69]	MSSM [70]	RPV [71, 72]	RS [73, 74]
$t \to Zu$	7×10^{-17}	–	–	$\leq 10^{-7}$	$\leq 10^{-6}$	–
$t \to Zc$	1×10^{-14}	$\leq 10^{-6}$	$\leq 10^{-10}$	$\leq 10^{-7}$	$\leq 10^{-6}$	$\leq 10^{-5}$
$t \to gu$	4×10^{-14}	–	–	$\leq 10^{-7}$	$\leq 10^{-6}$	–
$t \to gc$	5×10^{-12}	$\leq 10^{-4}$	$\leq 10^{-8}$	$\leq 10^{-7}$	$\leq 10^{-6}$	$\leq 10^{-10}$
$t \to \gamma u$	4×10^{-16}	–	–	$\leq 10^{-8}$	$\leq 10^{-9}$	–
$t \to \gamma c$	5×10^{-14}	$\leq 10^{-7}$	$\leq 10^{-9}$	$\leq 10^{-8}$	$\leq 10^{-9}$	$\leq 10^{-9}$
$t \to hu$	2×10^{-17}	6×10^{-6}	–	$\leq 10^{-5}$	$\leq 10^{-9}$	–
$t \to hc$	3×10^{-15}	2×10^{-3}	$\leq 10^{-5}$	$\leq 10^{-5}$	$\leq 10^{-9}$	$\leq 10^{-4}$

In Section 1.5.2 we summarize predictions for the size of flavor-changing top decays in the Standard Model and in various motivated models for new physics. In Section 1.5.3 we collect the current best limits on top FCNC decays from direct searches. In Section 1.5.4 we investigate the potential for future measurements at the LHC and ILC to constrain top FCNC.

1.5.2 Flavor-violating Top Decays

The branching ratios of flavor-violating decays of the top quark are controlled by the size of the flavor-violating partial width relative to the dominant top quark partial width $\Gamma(t \to bW)$. In Table 1-7 we summarize predictions for top FCNC branching ratios in the Standard Model and various motivated NP models. In the case of NP, the listed Br is intended as an approximate maximal value given ancillary direct and indirect constraints.

1.5.2.1 SM top FCNC

SM contributions to top FCNC are necessarily small, suppressed by both the GIM mechanism (which guarantees that the leading contributions are suppressed by both light quark masses and small CKM angles) and by the large total width of the top quark due to the dominant mode $t \to bW$ [75, 76]. This essentially guarantees that any measurable branching ratio for top FCNC decays is an indication of NP. The values in Table 1-7 are the from the updated numerical evaluation in [67]. Note that the results are very sensitive to the value of m_b as they scale as $m_b(m_t)^4$. The difference between decays involving the u quark and c quark arise from the relative factor $|V_{ub}/V_{cb}|^2$.

1.5.2.2 BSM top FCNC

Many models for new physics predict new contributions to top FCNC orders of magnitude in excess of SM expectations. Extended electroweak symmetry breaking sectors with two Higgs doublets (2HDM) lead

to potentially measurable FCNC. Parametric expectations are particularly large for 2HDM with tree-level flavor violation, for which flavor-violating couplings between Standard Model fermions and the heavy scalar Higgs H or pseudoscalar A are typically posited to scale with quark masses, $\propto \sqrt{m_q m_t / m_W^2}$, in order to remain consistent with limits on light quark FCNCs. Estimates in Table 1-7 are taken from [77, 68]. The flavor-violating decays arise at one loop due to the exchange of H, A, and the charged Higgs scalar $H^{\pm}$, with the rate depend on both the tree-level flavor-violating couplings between fermions and the heavy Higgses and the mass of the heavy Higgses themselves.

Even 2HDM with tree-level flavor conservation guaranteed by discrete symmetries predict measurable top FCNC due to loop processes involving the additional charged Higgs bosons. In this case the rate for flavor-violating processes depends on the mass of the charged Higgs and the angle $\tan\beta$ parameterizing the distribution of vacuum expectation values between the two Higgs doublets. In Type-I 2HDM, the branching ratios are typically small; the most promising candidate is $t \to gc \sim 10^{-8}$, with rates for $t \to hq$ several orders of magnitude smaller. In Type-II 2HDM, the leading contribution to $t \to hq$ is enhanced by $\mathcal{O}(\tan^4\beta)$ and may be considerable at large $\tan\beta$. The most optimistic cases are presented in Table 1-7, taken from [69] for Type I and Type II 2HDM. However, given that Higgs coupling measurements now constrain the allowed range of mixing angles in these 2HDM, the maximal rates for $t \to hq$ consistent with ancillary measurements are likely smaller.

In the MSSM, top FCNC arise at one loop in the presence of flavor-violating mixing in the soft mass matrices. Flavor violation involving the stop is much more weakly constrained by indirect measurements than flavor violation involving light squarks (particularly in the down-squark sector), allowing for potentially large mixings. However, rapidly-advancing limits on direct sparticle production have pushed the mass scale of squarks and gluinos to ≥ 1 TeV, rapidly suppressing loop-induced branching ratios. To obtain realistic estimates, in Table 1-7 we extrapolate the results of [70] to the case of $m_{\tilde{g}} \sim m_{\tilde{q}} = 1$ TeV. If R-parity is violated in the MSSM, top decays may also be induced at one loop by B or L-violating RPV couplings, though B-violating couplings dominate by an order of magnitude or more. For the estimates in Table 1-7, we extrapolate the results of [71, 72] to $m_{\tilde{q}} = 1$ TeV; for [71] we take their coupling parameter $\Lambda = 1$.

In models of warped extra dimensions (and their four-dimensional counterparts involving strong dynamics), top FCNC arise when Standard Model fermions propagate in the extra dimension with profiles governed by the corresponding Yukawa couplings. These non-trivial profiles lead to flavor-violating couplings between SM fermions and the Kaluza-Klein (KK) excitations of the SM gauge bosons. Such couplings are largest for the top quark, whose profile typically has the largest overlap with the gauge KK modes, and lead to flavor-violating couplings that depend on 5D Yukawa couplings and the mass scale of the gauge KK modes. Appreciable flavor-violating couplings involving the top quark and Higgs boson arise from analogous processes involving loops of fermion KK modes.

1.5.3 Current Limits

Limits on various top FCNC decays have progressed rapidly in the LHC era. We summarize the current best limits from direct searches in Table 1-8. CMS places the strongest limit on the decay $t \to Zq$ in the trilepton final state [78] using the full 8 TeV data set. ATLAS sets a sub-leading limit on $t \to Zq$ using a portion of the 7 TeV data set, but also sets the leading limits on $t \to gq$ via a search for s-channel top production [79] using 7 TeV data. The Tevatron still maintains best limits on some rare processes, in particular $t \to \gamma c$ from Run I [80] and $t \to$ invisible from Run II at CDF [81]. ZEUS maintains the best inferred limit on $t \to \gamma u$ [82]. The Tevatron and HERA limits on $t \to \gamma q$ are expected to be superseded by LHC limits using the 7+8 TeV data set, but to date no official results are available.

Table 1-8. *Current direct limits on top FCNC. (*) denotes unofficial limits obtained from public results. The q in the final state denotes sum over $q = u, c$.*

Process	Br Limit	Search	Dataset	Reference
$t \to Zq$	7×10^{-4}	CMS $t\bar{t} \to Wb + Zq \to \ell\nu b + \ell\ell q$	19.5 fb^{-1}, 8 TeV	[78]
$t \to Zq$	7.3×10^{-3}	ATLAS $t\bar{t} \to Wb + Zq \to \ell\nu b + \ell\ell q$	2.1 fb^{-1}, 7 TeV	[84]
$t \to gu$	5.7×10^{-5}	ATLAS $qg \to t \to Wb$	2.05 fb^{-1}, 7 TeV	[79]
$t \to gc$	2.7×10^{-4}	ATLAS $qg \to t \to Wb$	2.05 fb^{-1}, 7 TeV	[79]
$t \to \gamma u$	6.4×10^{-3}	ZEUS $e^{\pm}p \to (t \text{ or } \bar{t}) + X$	474 pb^{-1}, 300 GeV	[82]
$t \to \gamma q$	3.2×10^{-2}	CDF $t\bar{t} \to Wb + \gamma q$	110 pb^{-1}, 1.8 TeV	[80]
$t \to hq$	2.7×10^{-2}	CMS* $t\bar{t} \to Wb + hq \to \ell\nu b + \ell\ell q X$	5 fb^{-1}, 7 TeV	[83]
$t \to$ invis.	9×10^{-2}	CDF $t\bar{t} \to Wb$	1.9 fb^{-1}, 1.96 TeV	[81]

The recent discovery of the Higgs allows for limits to be set on $t \to hq$. Neither collaboration has yet placed an official limit on this process, but in [83] a limit was obtained on $t \to hq$ using the 7 TeV CMS multi-lepton search with 5 fb^{-1} of data, assuming Standard Model branching ratios for a Higgs boson with $m_h = 125$ GeV. Similar limits may be set using the CMS same-sign dilepton search. The CMS multi-lepton search has recently been updated to $5 \oplus 9$ fb^{-1} of $7 \oplus 8$ TeV data, and now includes b-tagged categories; this should substantially increase sensitivity to $t \to hq$ in the existing data set. While multi-lepton final states were used to set an initial bound, limits on $t \to hq$ from the $\gamma\gamma q$ final state are likely to be $\mathcal{O}(5\times)$ better than comparable multi-lepton limits.

Indirect limits on top FCNC may also be set through single top production, D^0 oscillations, and neutron EDM limits. At present these limits are not competitive with direct searches at the LHC for final states involving γ, Z [85], though they are comparable for final states involving h [86].

1.5.4 Projected Limits

Although current direct limits on flavor-violating top couplings do not appreciably encroach on the parameter space of motivated theories, future colliders should attain meaningful sensitivity. Here we will focus on the sensitivity of the $\sqrt{s} = 14$ TeV LHC after 300 and 3000 fb^{-1} of integrated luminosity, as well as the ILC operating $\sqrt{s} = 250, 500$ GeV with 500 fb^{-1} of integrated luminosity. The case of the $\sqrt{s} = 250$ GeV ILC is particularly interesting, since it possesses sensitivity to top FCNC through single-top production via a photon or Z boson.

1.5.4.1 LHC projections

At present, estimates of future LHC sensitivity to top FCNC arise from three sources: official projections from the ESG report [87]; approximate extrapolation from current searches at the 7 and 8 TeV LHC based on changes in luminosity, energy, and trigger thresholds; and dedicated study for the Snowmass process. Table 1-9 provides a summary of the projected limits at the 14 TeV LHC with 300 and 3000 fb^{-1} integrated luminosity.

Table 1-9. *Projected limits on top FCNC at the LHC. "Extrap." denotes estimates based on extrapolation as described in the text.*

Process	Br Limit	Search	Dataset	Reference
$t \to Zq$	2.2×10^{-4}	ATLAS $t\bar{t} \to Wb + Zq \to \ell\nu b + \ell\ell q$	300 fb^{-1}, 14 TeV	[87]
$t \to Zq$	7×10^{-5}	ATLAS $t\bar{t} \to Wb + Zq \to \ell\nu b + \ell\ell q$	3000 fb^{-1}, 14 TeV	[87]
$t \to \gamma q$	8×10^{-5}	ATLAS $t\bar{t} \to Wb + \gamma q$	300 fb^{-1}, 14 TeV	[87]
$t \to \gamma q$	2.5×10^{-5}	ATLAS $t\bar{t} \to Wb + \gamma q$	3000 fb^{-1}, 14 TeV	[87]
$t \to gu$	4×10^{-6}	ATLAS $qg \to t \to Wb$	300 fb^{-1}, 14 TeV	Extrap.
$t \to gu$	1×10^{-6}	ATLAS $qg \to t \to Wb$	3000 fb^{-1}, 14 TeV	Extrap.
$t \to gc$	1×10^{-5}	ATLAS $qg \to t \to Wb$	300 fb^{-1}, 14 TeV	Extrap.
$t \to gc$	4×10^{-6}	ATLAS $qg \to t \to Wb$	3000 fb^{-1}, 14 TeV	Extrap.
$t \to hq$	2×10^{-3}	LHC $t\bar{t} \to Wb + hq \to \ell\nu b + \ell\ell qX$	300 fb^{-1}, 14 TeV	Extrap.
$t \to hq$	5×10^{-4}	LHC $t\bar{t} \to Wb + hq \to \ell\nu b + \ell\ell qX$	3000 fb^{-1}, 14 TeV	Extrap.
$t \to hq$	5×10^{-4}	LHC $t\bar{t} \to Wb + hq \to \ell\nu b + \gamma\gamma q$	300 fb^{-1}, 14 TeV	Extrap.
$t \to hq$	2×10^{-4}	LHC $t\bar{t} \to Wb + hq \to \ell\nu b + \gamma\gamma q$	3000 fb^{-1}, 14 TeV	Extrap.

ATLAS has presented projections for sensitivity to $t \to Zq$ and $t \to \gamma q$ to the ESG report [87]. Using cut-based techniques, they anticipate $\mathrm{Br}(t \to \gamma q) < 8(2.5) \times 10^{-5}$ with 300 (3000) fb^{-1} at 14 TeV; using a more sophisticated discriminant, they project $\mathrm{Br}(t \to \gamma q) < 1.3 \times 10^{-5}$ at 3000 fb^{-1}. Similarly, using cut-based techniques, they anticipate $\mathrm{Br}(t \to Zq) < 2.2 \times 10^{-4}(7 \times 10^{-5})$ with 300 (3000) fb^{-1} at 14 TeV; using a more sophisticated discriminant, they project $\mathrm{Br}(t \to Zq) < 4 \times 10^{-5}$ at 3000 fb^{-1}. At present there is no public document from CMS with projections for 14 TeV sensitivity, nor are there official projections from either collaboration for $t \to gq$ or $t \to hq$.

Estimates for LHC sensitivity to $t \to gq$ and $t \to hq$ may be made by approximate extrapolation from current searches accounting for changes in luminosity, energy, and trigger thresholds. While crude, when applied to $t \to Zq$ this procedure agrees to within $\mathcal{O}(10\%)$ with the official ATLAS ESG projections and so provides a useful benchmark in lieu of detailed study. Applied to [83] by scaling with the luminosity and $t\bar{t}$ production cross section, this implies a 95% CL limit $\mathrm{Br}(t \to hq) < 2 \times 10^{-3}(5 \times 10^{-4})$ with 300 (3000) fb^{-1} at 14 TeV in the multi-lepton final state. Similarly applied to estimates [88] of sensitivity in the $\ell\nu b + \gamma\gamma q$ final state, this suggests a 95% CL limit $\mathrm{Br}(t \to hq) < 5 \times 10^{-4}(2 \times 10^{-4})$ with 300 (3000) fb^{-1} at 14 TeV. The extrapolation of $t \to gq$ is more delicate, since the process under study involves the tgq anomalous coupling in the production mode. Using the results from [89] to extrapolate the observed 7 TeV limit to 14 TeV, we find $\mathrm{Br}(t \to gu) < 4 \times 10^{-6}(1 \times 10^{-6})$ with 300 (3000) fb^{-1} at 14 TeV and $\mathrm{Br}(t \to gc) < 1 \times 10^{-5}(4 \times 10^{-6})$ with 300 (3000) fb^{-1} at 14 TeV.

Dedicated studies for Snowmass are under preparation. Specifically, improved estimates based on detailed studies for $\mathrm{Br}(t \to Zq)$ and $\mathrm{Br}(t \to \gamma q)$ are under preparation by ATLAS and should be available for Snowmass. Although there are no specific studies underway for $\mathrm{Br}(t \to hq)$ and $\mathrm{Br}(t \to gq)$ at 14 TeV, the ATLAS and CMS groups responsible for these searches at 7 and 8 TeV will provide improved estimates of limits at 14 TeV based on detailed extrapolation of current searches.

Table 1-10. *Projected 95% CL limits on top FCNC at the ILC.*

Process	Br Limit	Search	Dataset	Reference
$t \to Zq$	$5\,(2) \times 10^{-4}$	ILC single top, γ_μ ($\sigma_{\mu\nu}$)	500 fb^{-1}, 250 GeV	Extrap.
$t \to Zq$	$1.5\,(1.1) \times 10^{-4\,(-5)}$	ILC single top, γ_μ ($\sigma_{\mu\nu}$)	500 fb^{-1}, 500 GeV	[90]
$t \to Zq$	$1.6\,(1.7) \times 10^{-3}$	ILC $t\bar{t}$, γ_μ ($\sigma_{\mu\nu}$)	500 fb^{-1}, 500 GeV	[90]
$t \to \gamma q$	6×10^{-5}	ILC single top	500 fb^{-1}, 250 GeV	Extrap.
$t \to \gamma q$	6.4×10^{-6}	ILC single top	500 fb^{-1}, 500 GeV	[90]
$t \to \gamma q$	1.0×10^{-4}	ILC $t\bar{t}$	500 fb^{-1}, 500 GeV	[90]

1.5.4.2 ILC projections

At the ILC, sensitivity studies have focused on operation at $\sqrt{s} \geq 500$ GeV in order to probe both $e^+e^- \to t\bar{t}, t \to Xq$ as well as the single top process $e^+e^- \to tq$ due to, e.g., tZq or $t\gamma q$ anomalous vertices. Linear collider performance at $\sqrt{s} \geq 500$ GeV is studied in some detail in [90], which forms the basis for sensitivity estimates quoted here. The study [90] includes 95% CL estimates for various polarization options, including 80% e^- polarization and 45% e^+ polarization, close to the polarization parameters for ILC. In what follows we quote the 80%/45% polarization sensitivity, with the difference between 45% e^+ polarization and 30% e^+ polarization expected to lead to a small effect. We rescale the results of [90] to 500 fb^{-1} to match the anticipated ILC integrated luminosity; the results are presented in Table 1-10. Based on these estimates, ILC sensitivity at $\sqrt{s} = 500$ GeV should be comparable to LHC sensitivity with 3 ab^{-1} for $t \to Zq$ and $t \to \gamma q$. Since much of the sensitivity comes from single top production, the ILC is less likely to provide comparable sensitivity to $t \to hq$ and $t \to gq$.

The ILC also provides sensitivity to tZq and $t\gamma q$ anomalous couplings at $\sqrt{s} = 250$ GeV through single top production via the s-channel exchange of a photon or Z boson, $e^+e^- \to t\bar{c} + \bar{t}c$. In fact, production via Z exchange through the γ_μ vertex reaches its maximal cross section around 250 GeV and falls with increasing center-of-mass energy. Single top poduction cross sections through γ exchange or Z exchange with the $\sigma_{\mu\nu}$ coupling grow with increasing energy but are still appreciable at $\sqrt{s} = 250$ GeV . The disadvantage of $\sqrt{s} = 250$ GeV relative to higher center-of-mass energies is primarily the larger SM backgrounds to the single-top final state. In any event, this provides an intriguing opportunity for the ILC to probe new physics in the top sector even when operating below the $t\bar{t}$ threshold.

The prospects for constraining tZq and $t\gamma q$ anomalous couplings at $\sqrt{s} = 250$ GeV have not been extensively studied, but we may extrapolate sensitivity reasonably well based on the results of [91]. To obtain an estimate, we rescale the signal cross section after cuts for $e^+e^- \to t\bar{c} + \bar{t}c$ via anomalous couplings at $\sqrt{s} = 192$ GeV in [91] to $\sqrt{s} = 250$ GeV and conservatively assume the background cross sections are similar between $\sqrt{s} = 192$ GeV and $\sqrt{s} = 250$ GeV; in actuality the backgrounds should decrease with increasing center-of-mass energy. We assume a 60% b-tag efficiency and arrive at 95% CL estimates in Table 1-10.

1.5.5 Summary

Various well-motivated models predict branching ratios for top FCNC decays starting at $\sim 10^{-4} - 10^{-5}$, with the most promising signals arising in two-Higgs-doublet models and various theories with warped extra

dimensions. At present the LHC sensitivity to top FCNC decays is somewhat below the level predicted by motivated theories, with the notable exception of $t \to gu$ where searches for resonant single top production yield a limit $\mathcal{O}(10^{-4})$. However, future colliders (here the 14 TeV LHC and $\sqrt{s} = 250$ or 500 ILC) provide meaningful sensitivity to flavor-violating couplings of the top quark, of the same order as the largest rates predicted in motivated theories. With 3000 fb^{-1}, the 14 TeV LHC should provide sensitivities of order $\mathrm{Br}(t \to Zq) \sim 7 \times 10^{-5}$, $\mathrm{Br}(t \to \gamma q) \sim 3 \times 10^{-5}$, $\mathrm{Br}(t \to gq) \sim 1 \times 10^{-6}$, and $\mathrm{Br}(t \to hq) \sim 2 \times 10^{-4}$ at a single detector. With 500 fb^{-1} the 500 GeV ILC should provide sensitivities of order $\mathrm{Br}(t \to Zq) \sim 1 \times 10^{-5}$, $\mathrm{Br}(t \to \gamma q) \sim 6 \times 10^{-6}$, potentially improving upon LHC limits and providing useful complementarity. Intriguingly, even at $\sqrt{s} = 250$ GeV the ILC should provide meaningful sensitivity to $t \to Zq, \gamma q$ of similar order as the high-luminosity LHC.

Should additional resources be available before the conclusion of the Snowmass process, the highest priorities are more detailed studies of sensitivity to $t \to hq, t \to gq$ at LHC and $t \to Zq, t \to \gamma q$ via single top production at the $\sqrt{s} = 250$ GeV ILC. While the current estimates for these channels contained in this report should be valid to $\mathcal{O}(10 - 50\%)$, the importance of these channels and the corresponding considerable reach at LHC and initial-stage ILC merit more detailed feasibility studies.

There are a variety of possible scenarios in which top FCNC sensitivity of the LHC and ILC could lead to the discovery and identification of physics beyond the Standard Model. An intriguing scenario is the observation of the flavor-violating decay $t \to Zc$ at the LHC with a branching ratio on the order of 10^{-5}, at the limit of the projected high-luminosity reach. Such a branching ratio would be some nine orders of magnitude larger than the Standard Model expectation and a clear indication of new physics. At the LHC the primary backgrounds to this channel are Standard Model diboson ZZ and WZ production with additional jets, with a lesser component from Z+jets and rarer SM top processes ttW and ttZ. The diboson backgrounds are fairly well understood and in excellent agreement with simulation, and even the rare contributions from ttW and ttZ will be well-characterized by the end of the high-luminosity LHC run, making the observation of $t \to Zc$ fairly reliable.

Such a signal would be consistent with new physics arising from, e.g., warped extra dimensions, a composite Higgs, or a flavor-violating two-Higgs-doublet model. Ancillary probes of FCNC processes become crucial for validating the signal and identifying its origin. Some of the most important probes are the rare decays $t \to gc, t \to \gamma c$, and $t \to hc$, which have similar reach at the high-luminosity LHC. In the case of warped extra dimensions or a composite Higgs, the corresponding branching ratios for $t \to gc$ and $t \to \gamma c$ are orders of magnitude below the sensitivity of the LHC, but the branching $t \to hc$ may be as large as 10^{-4}, within the reach of high-luminosity LHC. Thus a signal in $t \to Zc$ with a tentative signal in $t \to hc$ but no other channels would be indicative of warped extra dimensions or a pseudo-Goldstone composite Higgs. Rates of this magnitude would also suggest e.g. a relatively low KK scale, so that complementary direct searches for heavy resonances would play a crucial role in testing the consistency of this possibility. In contrast, in flavor-violating two-Higgs-doublet models, a visible $t \to Zc$ signal can be accompanied by comparable signals in $t \to gc$ and $t \to hc$, allowing this scenario to be similarly differentiated.

Instrumental complementary information can be provided by the ILC. Projections of the $\sqrt{s} = 500$ GeV ILC with 500 fb^{-1} place its sensitivity to $t \to Zq$ coming from a γ^μ spin structure at the level of 10^{-4}, but sensitivity to $t \to Zq$ in single top production from a $\sigma^{\mu\nu}$ structure at $\sim 10^{-5}$. The observation of comparable $t \to Zc$ signals at the LHC and ILC could then favor a $\sigma^{\mu\nu}$ coupling and rule out candidate explanations such as warped extra dimensions.

1.6 Probing physics beyond the Standard Model with top quarks

The top quarks should provide a sensitive probe for physics beyond the Standard Model, based on the following rough argument. The presence of new physics at the TeV scale is very well-motivated by its role in solving the Planck-weak hierarchy problem of the SM. Namely, such new particles (NP) can prevent quantum corrections from dragging the Higgs boson mass (and hence its vev, i.e., the weak scale) all the way up to Planck scale. Such NP must then necessarily couple to the Higgs boson. However, because the top quark has largest coupling (among SM particles) to Higgs boson, quantum/loop corrections due to the top quark are the largest/dominant source of destabilization/divergence in Higgs mass. Thus, such NP also couples preferentially to (or is associated with) the top quark (among the other SM particles).

In this section, we focus on NP decaying into top-like final states. The studies performed for Snowmass process can be grouped into the following three categories: searched for stops, top-partners and $\bar{t}$ resonances and these are described in turn below. NP effects also lead to rare decays which are discussed in section 1.5.

1.6.1 Stops

Supersymmetry (SUSY) is perhaps the most popular solution to the Planck-weak hierarchy problem of the SM. It involves addition of a *superpartner* for every particle of the SM, with a spin differing by 1/2-unit from that of the corresponding SM particle. While in general superpartner masses in SUSY models are very model-dependent, naturalness strongly suggests that the scalar partners of the top quark, or *stops*, should have masses around the week scale The reason is that the stops cancel the largest divergence in the Higgs mass squared parameter, namely that from SM top loop (as mentioned earlier). This makes stops a prime target for LHC searches. The results of such searches are typically presented in terms of the "vanilla stop" simplified model, which contains two particles, a stop $\tilde{t}$ and a neutralino LSP $\tilde{\chi}^0$. The stop is assumed to decay via $\tilde{t} \to t\tilde{\chi}^0$ with a 100% branching ratio. Within this model, the current "generic" bound on the stop mass is about 700 GeV [92, 93]. However, it must be emphasized that lighter stops are still allowed. In particular: (a) If $m(\tilde{\chi}^0) > 250$ GeV, stops of any mass are allowed; (b) in the "off-shell top" region, $m_t > m(\tilde{t}) - m(\tilde{\chi}^0) > m_W$, stops above 300 GeV are allowed; (c) in the "compressed" region, $m(\tilde{t}) \approx m(\tilde{\chi}^0) + m_t$, stops of any mass are allowed (this includes the particularly challenging "stealthy" region, $m(\tilde{t}) \approx m(t) \gg m(\tilde{\chi}^0)$); and (d) in the "squeezed" region, $m(\tilde{t}) - m(\tilde{\chi}^0) < m_W$, stops of any mass are allowed. In all these regions, kinematics of stop production and decay yields events with little missing transverse energy (MET), reducing the efficiency of LHC searches. The future experiments have a two-fold task: improve the reach on $m(\tilde{t})$ for generic spectra; and explore the special regions listed above. LHC will clearly play a leading role. However, it should be emphasized that in any of the special regions, stops can still be within the kinematic reach of the ILC, at $\sqrt{s} = 500$ GeV or 1 TeV. In this case, the ILC could play a crucial role in discovering the stops and precisely determining their properties, *e.g.* spin, masses and the mixing angle.

Both ATLAS and CMS have presented estimates of the discovery reach of LHC-14 and HL-LHC in the vanilla stop model, extrapolating the present 1-lepton search [94, 95]. For a "generic" spectrum, stops up to approximately 800 (900) GeV can be discovered, at a 5-σ level, with 300 fb^{-1} (3 ab^{-1}) integrated luminosity. However, significant gaps in the coverage of this search remain: for example, no discovery is possible for the LSP mass above 500 GeV, as well as in the compressed and stealthy regions, even at HL-LHC. It is clear that novel search strategies would be needed to cover these regions.

1.6.1.1 Stealth stops

Two studies of such strategies were contributed to our working group. Han and Katz [96] focused on the stealthy stop region, which is particularly challenging since, unlike the region with a heavy neutralino, no significant MET is generated even in the presence of ISR jets. The challenge is to distinguish $\tilde{t}\tilde{t}^*$ events from a much larger $t\bar{t}$ background. Two methods to achieve this task have been studied: (a) using spin correlations, which are present in $t\bar{t}$ but not in $\tilde{t}\tilde{t}^*$ events, due to $\tilde{t}$ being a scalar particle [97]; and (b) using an m_{T2} cut in dileptonic event sample [98]. It was found that, using spin correlations, LHC-14 with 100 fb^{-1} of data will be able to discover the stealthy stop at the 5σ level, assuming the stop mass of 200 GeV. To check the performance of the m_{T2} method, the authors plot the m_{T2} distibutions in Fig. 1-4 for the three data samples that were generated. Applying a cut of $m_{T2} > 95$ GeV, we obtain ~ 250 top events, ~ 270 right-handed stop events, and ~ 40 left-handed stop events. Assuming a 15% systematic error, the m_{T2} method will be able to discover right-handed stops in the $(185, 195)$ GeV window, while the sensitivity to the left-handed stop is poor due to the absence of a long m_{T2} tail in the signal in this case.

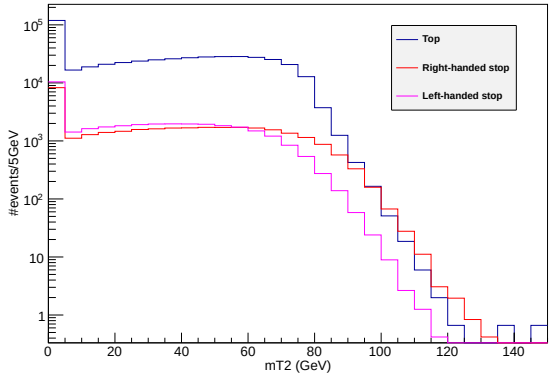

Figure 1-4. *The m_{T2} distributions for LHC14 with 100 fb^{-1} data.*

The second study, by Delannoy *et.al.* [99], analyzed the possibility of using the vector boson fusion stop production channel, which provides additional jets that could be used to tag the events with stealthy, compressed, or light stops. Fig. shows the distributions (normalized to unity) of invariant mass of the two leading jets of the sample for $\tilde{t}$ pair production by VBF processes and the main sources of background at LHC14. It was found that, for example, the LHC-14 with 300 fb^{-1} of data will be able to probe the scenario with $m(\tilde{t}) = 233$ GeV and $m(\tilde{\chi}^0) = m(\tilde{t}) - m_t$, at a 3σ level.

1.6.1.2 Gluino-initiated stop production

In addition to stops, naturalness also strongly motivates a light gluino, constraining its mass through the one-loop QCD correction to stop mass. A rough naturalness bound is $m(\tilde{g}) < 2m(\tilde{t})$ [100]. This motivates considering a simplified model with gluino, stop and an LSP, with a decay $\tilde{g} \to t\bar{t}$+MET. Assuming that this decay proceeds via an off-shell stop and has a 100% branching ratio, LHC-8 searches rule out gluino masses up to about 1.3 TeV, provided that the LSP mass is below 500 GeV [101, 102]. Extrapolating the search in the all-hadronic channel, CMS estimates a 5σ discovery reach of 1.7 TeV at LHC-14 with 300 fb^{-1} of data [95]. For gluino masses above TeV, "boosted" (relativistic in the lab frame) tops become increasingly common in $\tilde{g}$ decays. In this regime, boosted top tagging techniques [103], developed and tested at the LHC

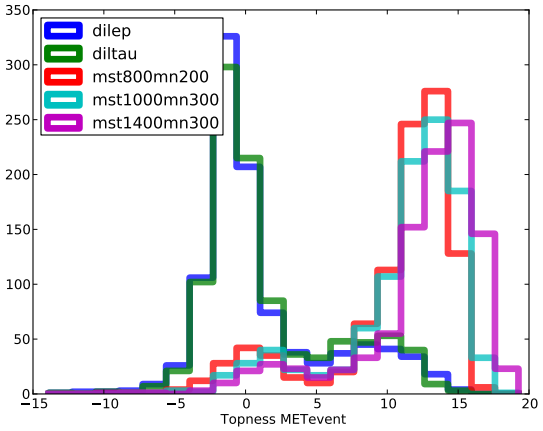

Figure 1-5. *Unit-normalized topness distributions for events passing preselection cuts as described in the text. Good separation is seen between the two dominant backgrounds (dileptonic top, blue, solid; leptonic-tau top which has one ℓ, one τ top, green, solid) and several simplified stop models ($m_{\tilde{t}_1}$, $m_{\chi_1^0}$)=(800, 200, red), (1000, 300, light blue), and (1400, 300, purple).* **fix legend**

for non-SUSY applications, can be used to provide a novel handle to search for SUSY. A preliminary study (with no detector simulation) suggests that gluinos with masses up to 1.4 TeV can be discovered at the LHC-14 with only 10 fb^{-1} of data, using top-tags in combination with more traditional cuts in all-hadronic events [104].

1.6.1.3 Including more electroweak particles

Another well-motivated extension of the vanilla stop simplified model is to add a chargino $\tilde{\chi}^{\pm}$, with $m(\tilde{\chi}^{\pm}) < m(\tilde{t})$. This is also motivated by naturalness, since the charged Higgsino mass is controlled by the μ parameter which cannot be far above 100 GeV in natural SUSY models. This simplified model has the possibility of *asymmetric* stop events: *e.g.* $pp \to \tilde{t}\tilde{t}^*, \tilde{t} \to t\tilde{\chi}^0, \tilde{t}^* \to b\tilde{\chi}^{\pm}$. A study of the LHC sensitivity to this signal was performed by Graesser: for more details, see [105]. The proposed search uses the 1-lepton+MET channel, and relies crucially on the "topness" variable, introduced in [106] as a general tool to suppress the $t\bar{t}$ background in this channel. Distributions for topness are shown in Fig. 1-5. It was found that 5σ discovery is possible at LHC-14 with 300 fb^{-1} for stop masses up to about 800 GeV, if $m(\tilde{\chi}^0)$ is below about 300 GeV. With 3000 fb^{-1}, the discovery reach extends to stop masses about 1.2 TeV for light $\tilde{\chi}^0$. A related simplified model was used in the study by Dutta *et.al.* [107]. Motivated by the "well-tempered neutralino" dark matter scenario [108], this study considered a spectrum with light bino and Higgsino, leading to three neutralino and one chargino states at the bottom of the SUSY spectrum (it was assumed that all these states are lighter than the stop). The analysis focused on the dilepton signature, where the leptons can come either from top decays or from $\chi^0_{2,3} \to Z\chi^0_1$. It was found that [to be continued].

1.6.1.4 R-parity violation

Yet another interesting scenario is R-parity violating (RPV) supersymmetry, where a stop can decay via $\tilde{t} \to \bar{b}\bar{s}$ induced by the UDD superpotential operator. This scenario emerges naturally from models with minimal flavor violation [109, 110]. Direct stop production in this case yields all-hadronic final states, and

does not provide a promising search channel. However, just as in conventional SUSY, naturalness strongly suggests the presence of relatively light gluinos. Gluino decays via cascades involving stops, $\tilde{g} \to \tilde{t}t, \tilde{t} \to 2j$, may be observable, even though they do not produce large MET. If $\tilde{g}$ is Majorana, as in simplest SUSY models, such decays can provide a striking same-sign dilepton (SSDL) signature. Current SSDL searches already rule out gluinos up to 800 GeV, independent of the stop mass, in the RPV scenario [111]. At LHC-14 with 100 fb^{-1} of data, the projected reach of this search is $1.3-1.4$ TeV, again approximately independent of the stop mass [111]. This estimate includes an improvement in sensitivity due to an additional requirement of one or two massive jets. (The massive jets can be either due to boosted stop decays, or to accidental mergers of neighboring jets in a high jet multiplicity signal event.) An alternative is a search in a single-lepton channel, which has a higher rate and applies to both Majorana and Dirac gluinos [112]. In this case, the requirement of stop mass reconstruction from jet pairs can be used as an additional handle to suppress backgrounds. An estimate of the potential of this search at LHC-14 was contributed by A. Katz [113]. It was found that this search will be sensitive to gluino masses up to XXX TeV.

1.6.2 Top-partners

Alternative solutions to the Planck-weak hierarchy problem are provided by models such as little Higgs and composite Higgs (often realized in/conjectured to be dual to the framework of a warped extra dimension, following the AdS/CFT correspondence). In these scenarios, the divergence in Higgs mass squared parameter from SM top loop is cancelled by a new *fermions* which are vector-like under the SM gauge symmetries, in particular, they are color triplets with electric charge 2/3 (i.e., same as the SM top), hence these new particles are dubbed "top-partners". Such particles can also arise in other extensions of the SM so that it i useful to follow a model-independent, simplified approach in studying their signals. The top-partners can be produced via QCD interactions in pairs or singly, the latter resulting from coupling of top-partner to SM top/bottom, as needed to cancel the SM top divergence in Higgs mass squared parameter. Both processes have been studies as part of Snowmass process.

Based on the $SU(2)_L$ gauge symmetry of the SM, the top-partners are often accompanied by "bottom-partners" Finally, in some composite Higgs models, an extension of the EW symmetry group (from that in the SM) is motivated by avoiding constrains from $Zb\bar{b}$: this results in the appearance of color triplet, but charge 5/3 particles (in addition to the above top/bottom partners).

Once produced, these top/bottom-partners and charge-5/3 fermions decay into a top-like final state. Some details of all these studies are given in what follows (for more information, see the corresponding Snowmass whitepapers).

1.6.2.1 Pair production of top-partners

The authors of this study are S. Bhattacharya, U. Heintz and M. Narain. They consider decays of the this top-partner into three possible decay modes: bW, tH and Zt. The interesting feature is that, in the limit of a heavy top-partner, the decay modes are equally shared by these three modes (following the principle of Goldstone equivalence). The decay topology of the top-partner leads to the presence of multiple W and Z bosons in the final state that produce leptons and multiple b-jets. The Higgs (at 125 GeV) is forced to decay into either $b\bar{b}$ or W^+W^- since these are the modes that have the highest branching fraction and lead to final states that are sensitive to the analysis strategy.

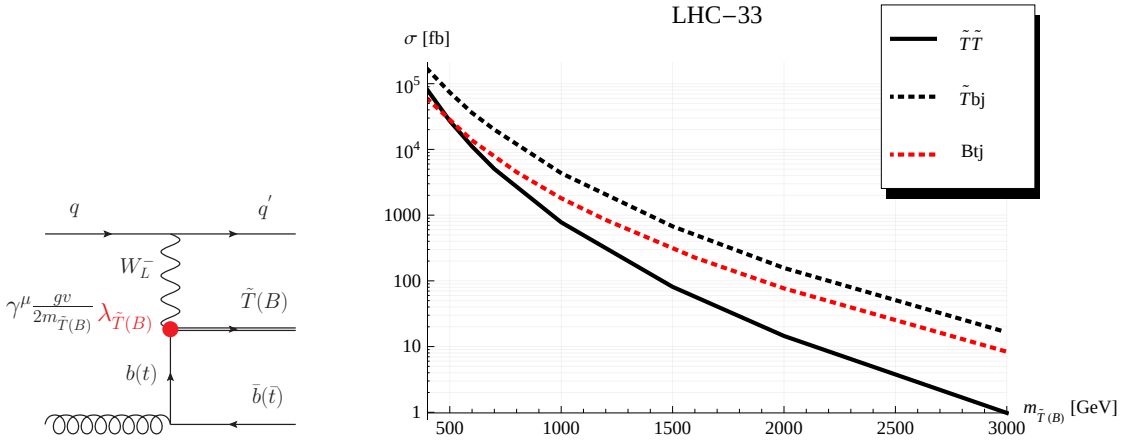

Figure 1-6. *Single production of top- and bottom- prime VLQs (left). VLQ cross sections at the 33 TeV LHC. Dotted curves correspond to single-productions for $\lambda_\chi = 3$ (right).*

The study focuses on channels with at least two leptons. For the case of opposite-sign dileptons, the signal and background distributions of relevant variables are shown in Fig... Reference [114] contains more details of the analysis.

1.6.2.2 Single production of top/bottom-partners

This study was done by T. Andeen, K. Black, C. Bernard, T. Childress, T, L Dell'Asta and N. Vignaroli. The single production proceeds by means of the top/bottom-partners electroweak effective couplings to a weak boson and a SM quark (denoted by λ_χ): see Fig. 1-6 (left). These production mechanisms have larger rates than those of pair productions for heavier top/bottom partners. Moreover, analyses of single-production channels might permit the measurement of the effective couplings λ_χ. Fig. 1-6 (right) shows the cross sections at the 33 TeV LHC for top/bottom-partner (and charge-5/3) pair production and for single production of top-partner and bottom partner (which is the same as for charge-5/3), for $\lambda_\chi = 3$. The top-partner single-production, that proceeds via the intermediate exchange of a bottom quark has a rate significantly higher than those of bottom partner and charge-5/3 productions, which are mediated by the exchange of a top.

As mentioned above, the top-partner can decay into one of three possible final states at tree level: ht, Zt and Wb. Since the W + jet backgrounds are considerable for the third mode, here the authors focus on the first two decay modes. The basic idea is to reconstruct the top-partner mass: for more details, see reference [115]. In the ht channel, the authors estimate that (based on statistics only) that one experiment should be able to see a 5 σ discovery of a top-partner in the single production channel up to approximately 1750 GeV and exclude a top-partner up to a mass around 2200 GeV (both at LHC 33). [Note that the authors will add systematics, LHC 14 and different pileup (and similarly for the Zt channel) soon.]

1.6.2.3 Pair production of bottom-partners

This study is due to E. Varnes. All samples used for these studies were processed with the DELPHES fast detector simulation, using the generic "Snowmass detector" parameters. The background samples were generated in bins of H_T. Signal samples were generated with MAD GRAPH v1.5.10, with bottom-partner masses of 1.0 and 1.5 TeV. These events were then processed by PYTHIA8 to simulate decays and hadronization. The decays of the bottom-partners was forced to Wt, Zb, or Hb such that each of the six possible final states ($W^-tW^+\bar{t}$, $W^-tZ\bar{b}$, $W^-tH\bar{b}$, $ZbZ\bar{b}$, $Z\bar{b}Hb$, or $HbH\bar{b}$) from pair production of bottom-partners were generated as separate samples. There samples were then processed by DELPHES with 0, 50, or 140 minimum-bias events overlaid on average to simulate the eftects of pileup.

The following pp collider scenarios are considered: LHC14 and 33, each with 300 fb^{-1} (average of 50 pileup events) and with 3000 fb^{-1} (an average of 140 pileup events). There is an interesting signal of same-sign dilepton in some cases here. More details can be found in reference [116].

1.6.2.4 Pair production of Charge-5/3

The interesting feature of charge-5/3 vector-like fermion is that its decay gives rise to *same*-sign dileptons, i.e., final state is $tW^+ \to bW^+W^+$, followed by leptonic decays of both W's. The potential for discovery of such a fermion as a function of the luminosity was analyzed by A. Avetisyan and T.Bose and exclusion limits are presented using integrated luminosities of 300 fb^{-1} and 3000 fb^{-1} at center-of-mass energies of 14 and 33 TeV.

All samples used in this study are generated using MadGraph 5 and simulated using Delphes 3.0.9. For the backgrounds, the MadGraph generation is done in bins of the sum of transverse energy of all MadGraph-level particles in the event. The detector used as input to the simulation of both signal and background samples is the Snowmass Combined LHC detector. Two pileup scenarios are considered for each center-of-mass energy: one with 50 mean interactions per bunch crossing and one with 140 such interactions.

Signal samples are generated with the charge-5/3 mass varied in intervals of 100 GeV. The mass in 14 TeV samples ranges from 700 GeV to 1600 GeV while for 33 TeV samples, it varies from from 700 GeV to 2200 GeV. The principal same-sign backgrounds are $\tilde{t\bar{t}}W$, $t\bar{t}Z$, $W^{\pm}W^{\pm}$ and the various combinations of triboson backgrounds (e.g. WWW, WWZ, etc.). In addition, $t\bar{t}$ and $Z + Jets$ backgrounds will be used to estimate the contribution due to misidentifying the charge of one of the electrons.

In addition to using the same-sign dileptons as a handle to reduce background for the signal, the presence of boosted W and top (identified by special tagging techniques) and (in general) large transverse momentum decay products (in turn, due to heaviness of charge-5/3 fermion) can help. For more details, see reference [117].

At the LHC14 with 300 fb^{-1}, the (preliminary) discovery reach was found to be 1.15 TeV, whereas exclusion is 1.25 TeV.

1.6.3 $t\bar{t}$ resonances

In composite Higgs models (and their warped extra dimensional duals), there are typically bosonic new particles which decay dominantly into $t\bar{t}$. And, they are favored to be rather heavy (a few TeV) due to

the constraints from various precision tests. Thus, the resulting top quarks are boosted, requiring special identification techniques. Other extensions of the SM can also feature such resonances.

Two such studies of $t\bar{t}$ resonances were done as part of the Snowmass process and are discussed in what follows. Note that there is also overlap with discussion in the following section of this report.

1.6.3.1 Search for $t\bar{t}$ resonances at future hadron colliders using jet mass/Snowmass top-tagger

The authors of this study are Aaron Effron, Johannes Erdmann, Tobias Golling and Chris Pollard. They present the expected sensitivity to a leptophobic topcolor Z' particle [118] and a Kaluza-Klein (KK) gluon in the Randall-Sundrum (RS) warped extra dimension model [119], assuming the upgraded LHC will deliver an integrated luminosity of 3000 fb^{-1} at $\sqrt{s} = 14$ TeV, and they compare this result to the expected sensitivity of a 300 fb^{-1} dataset.

The Z' signal samples are generated at invariant masses of 2, 3, 4 and 5 TeV using Pythia. The $t\bar{t}$ and QCD multijet background samples for the all-hadronic analysis were generated with Herwig++, where a minimum p_{T} requirement on the two highest-p_{T} partons of 650 GeV was required at generator level. All samples were overlaid with simulated minimum-bias events corresponding to three pile-up scenarios with an average number of interactions per bunch-crossing of 0, 50 and 140. The samples were reconstructed using the DELPHES fast detector simulation. All cross sections were obtained at LO from the respective generators.

Both leptonic and all hadronic decays of the tip quark are considered. In order to identify the boosted tops, the authors make use of the top ("fat")-jet mass distribution peaking at the top mass and the distribution of di-subjet mass peaking at the W mass. For the all-hadronic analysis, the authors have updated to the most recent Delphes setup, which includes a top-tagger as developed for Snowmass process by James Dolen and John Stupak. For more details, see reference [120].

Fig.... shows the reconstructed Z' mass distribution after selection, where the Z' signal is shown on top of the different background contributions in the single lepton (a) and in the all-hadronic (b) channel. In the lepton plus jets channel the Z' mass is reconstructed using the four-vectors of the lepton, the selected small-radius (R) jet, the selected large-R jet, and the neutrino. In order to determine the p_Z of the neutrino, a W mass constraint is applied to the E_T^{miss}-lepton system. In the hadronic channel, the Z' mass is reconstructed using the four-vectors of the two highest-p_{T} large-R jets.

The systematic uncertaines that are expected to be dominating were carefully evaluated for the analyses in the single lepton and in the all-hadronic channel. The $t\bar{t}$ invariant mass spectra of events which pass the selections are used to distinguish the SM prediction from the signal templates. The Bayesian Analysis Toolkit is used to determined the 95% CL upper limits on the signal cross section for each mass point given the SM mass spectrum and that of a given signal model. The signal cross section is taken to have a constant prior, while a gaussian prior is used for the systematic uncertainties. Given the upper limits on signal cross sections, the authors expect to exclude XXX.

1.6.3.2 Searches for RS KK-gluons with the Template Overlap Method in the high end of boosted top regime

The study reported in this section was performed by Mihailo Backovic and Seung Lee. Using RS KK-gluon as an example, estimate the discovery potential for top pair resonance in the future 14 and 33 TeV LHC experiment using the Template Overlap Method (TOM) [121].

TOM has been extensively studied in the past in the context of theoretical studies of boosted tops and boosted Higgs decays [122], as well as used by the ATLAS collaboration for a boosted resonance search [123]. The method is designed to match the energy distribution of a boosted jet to the parton-level configuration of a boosted top decay, with all kinematic constraints taken into account. Because our analysis focuses on events in which one top decays hadronically and the other semi-leptonically, we employ two different formulations of TOM. The hadronic TOM, which is designed to tag the fully hadronic decays of the top, and the leptonic TOM, designed to take into account decays with missing energy [3]. The latter is particularly useful in compensating for the loss of rejection power due to the absence of efficient b-tagging methods at high p_T.

Low susceptibility to intermediate levels of pileup (i.e. 20 interactions per bunch crossing), makes TOM particularly attractive for boosted top analyses at the LHC. Refs. showed that the ability of TOM to tag the top jets is nearly unaffected even at 100 interactions per bunch crossing, with the W+jets mistag rate changing by as little $\approx 10\%$ at 20, thus nearly eliminating the need for pileup subtraction/correction at intermediate pileup levels.

For more details about how the TOM is used in this study, see reference [124]. The first Snowmass benchmark point the authors consider is the Case 1 RS KK gluon (Right handed, near the brane) with$M_{G'_{KK}} = 3$ TeV. They generated the data using MadGraph + Pythia, with CTEQ6M parton distribution functions at $\sqrt{s} =$ 14 TeV, while jet clustering is performed using the FastJet implementation of the anti-k_T algorithm. Note that they did not impose an implicit mass window on the top jets, and instead rely on the intrinsic mass filtering ability of TOM as a pileup insensitive alternative.

Fig. 1-7 show the results of the overlap analysis on the signal events. In both cases the method is able to tag the signal tops with a high efficiency, whereas the peak at low overlap values can be attributed to the events in which one of the top decay products is outside the jet cone, thus producing a fat-jet with lower mass (*background will be shown later*).

The authors then consider other Snowmass benchmark points for Case 1 RS KK gluon (Right handed, near the brane) with$M_{G'_{KK}} = 5$, 6 and 8 TeV at $\sqrt{s} = 14$, 33 TeV, and show how far can 14 TeV with 300 fb^{-1} vs 3000 fb^{-1} and 3000 fb^{-1} 33 TeV LHC reach for higher resonance searches (*to be done*).

1.7 Top Algorithms and Detectors

Since the discovery of the top quark, the Tevatron has made great progress in our understanding of this massive quark, including its production, decays, mass and width, and other properties. (citations or bring this whole intro out into the main text body?). Now, with the first run of the LHC completed, the long-awaited measurements of top quarks and their properties by ATLAS [125] and CMS [126] have proven the LHC to be the world's top factory. The Standard Model (SM) top-quark studies at the LHC include[4]

[3] We use the TemplateTagger v.2.0 of TOM for both the hadronic and the leptonic formulations.

[4] We give only the most representative or recent references which are only needed to make our point, without attempt to collect a comprehensive list of references from ATLAS and CMS.

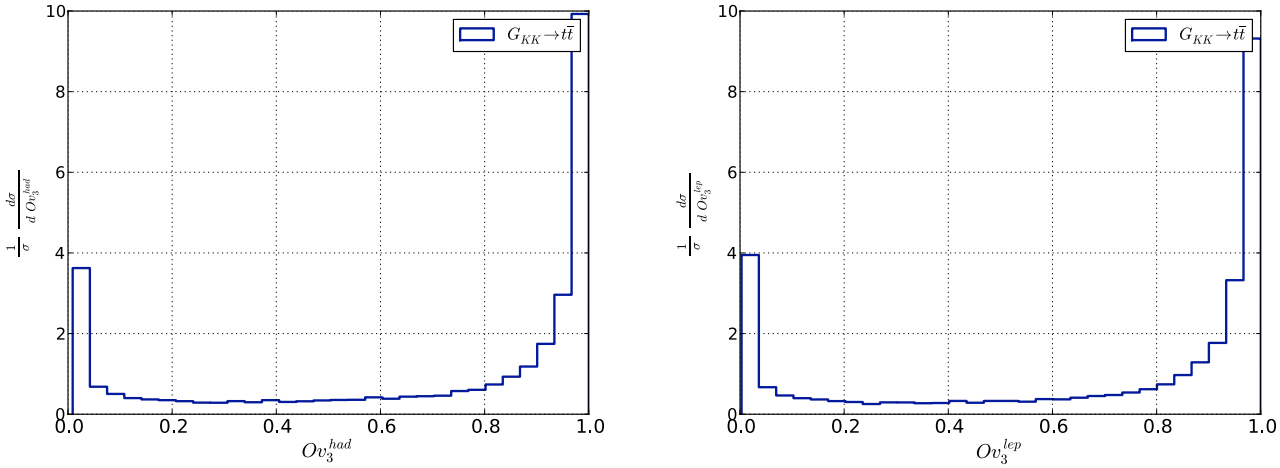

Figure 1-7. *Template Overlap analysis of the G'_{KK} events at $\sqrt{s} = 14$ TeV with $M_{G'_{KK}} = 3$ TeV. The left panel shows the distribution of Ov_3^h, while the right panel shows the corresponding Ov_3^l (for the definition of these variables, see [124]). The analysis assumes no implicit cut on the top mass or pileup contamination.*

reconstruction of the total and differential $t\bar{t}$ cross sections [127, 128, 129, 130, 131, 132, 133, 134, 135] top-quark mass measurements [136, 137, 138], cross sections of invariant masses of $t\bar{t}$ pairs, charge asymmetry [39] and single-top measurements [139].

1.7.1 Threshold Top Production

Top-quark reconstruction near threshold, at low transverse energies, is limited by a number of factors that determine total systematic uncertainty, including: a) jet-energy scale uncertainty which typically accounts for 50% of the overall uncertainty on traditional top-quark measurements based on jets; b) jet-energy resolution uncertainty; c) b-tagging efficiency uncertainty and mistag rates; and d) uncertainty on missing transverse-energy reconstruction. This indicates that any further progress in precision top measurements near threshold involving jet reconstruction can only come from a better understanding of low-p_T(jet) jets (typically, $25 < p_T(\text{jet}) < 50$ GeV jets) and $b-$tagging.

Future plans for a high-luminosity LHC upgrade only complicates this picture. Moving beyond $\langle\mu\rangle \geq 100$ pileup events per bunch crossing will have a negative impact on many final-state observables, the most vulnerable of which are low-p_T jets and b-tagged jets due to their large associated systematics. Studies of this scenario [140] were performed for the Snowmass CSS for pp collisions at a center-of-mass energy of $\sqrt{s} = 14$ TeV. Top quarks were modeled using the `PYTHIA8` [141] and `HERWIG++` [142] Monte Carlo (MC) models. The MC samples were processed through a fast detector simulation based on the `Delphes` 3.08 framework [143] assuming the Snowmass detector geometry. The samples are available from the Snowmass web page [144]. Jets were reconstructed with the `FastJet` package [145] using the the anti-k_T algorithm [146] with the distance parameter $R = 0.5$. For these studies, we ignored out-of-time pileup.

These high-luminosity MC simulation studies have shown that in general, pileup events: 1) shift jet transverse energies by approximately 50 (120) GeV for $\langle\mu\rangle = 50$ (140) scenarios, adding about one additional GeV for each pileup event; 2) smear jet transverse momenta; and 3) create a flux of low-p_T fake jets. Figure 1-8(a)

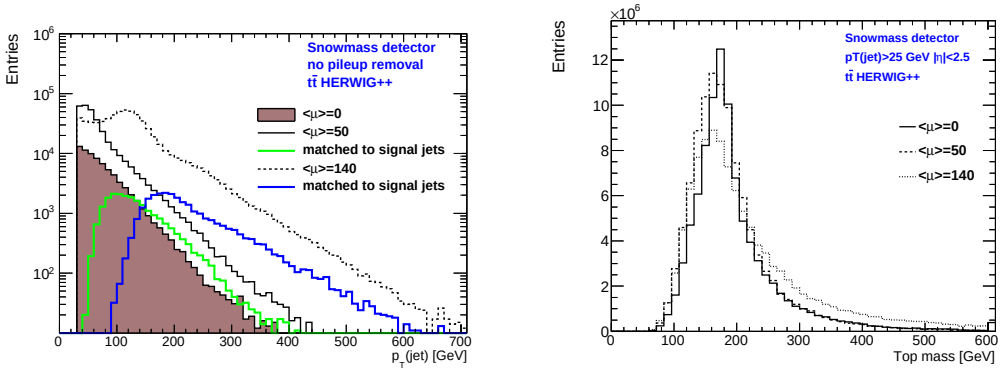

(a) (b)

Figure 1-8. *(a) Plots of jet p_T distributions for different pileup scenarios using the* Delphes *simulation. Also shown are only the jets matched to the top quarks in the event for each pileup scenario, demonstrating the large effect of additional pileup events on top quark reconstruction. (b) Reconstructed top quark masses from trijets by requiring at least four jets with $p_T > 25$ GeV and $|\eta| < 2.5$, and at least one of the jets must be tagged by a b-tagging algorithm.*

shows the effect of these pileup scenarios on the jet p_T distribution. One consequence of the energy shift is that for the selection of top quark signal jets, a pileup subtraction technique should correct the signal jets by 200-400%, leading to larger uncertainties compared to previous analyses. Uncertainties due to pileup will become dominant, and are expected to increase by a factor of two or more. the highest luminosities. As an example, a 2% jet-energy scale uncertainty for a jet measurement without pileup translates to a 3%(5%) uncertainty in case of 50 (140) pileup scenario.

Since uncertainties in jet resolution, jet energy scales, and b-tagging dominate in top quark measurements, most inclusive SM top quark studies will suffer at high luminosities, particularly those that use standard top reconstruction methods based on jets. We estimate that systematic uncertainties for the SM top measurements will increase by a factor 1.5(2.5) for the 50(140) pileup scenario. Data-driven techniques may improve the assessment of the jet energy scale compared to this projection, but it is unlikely that this can make a significant difference to the above conclusion. It is doubtful that precision top-quark measurements based on jets will have uncertainties similar to or better than the corresponding theoretical error estimate.

Standard top mass measurements will also be degraded by the high pileup in high-luminosity runs: A Delphes MC study presented in [140] shows that using the trijet mass for top-reconstruction is strongly affected by pileup events even when using particle-flow methods and pile-up subtraction techniques. Figure 1-8(b) shows the reconstructed top mass using a procedure similar to the one discussed in [147]. It was also observed [140] that the trijet mass for top-reconstruction strongly depends on p_T(top) (due to large jet multiplicity from ISR/FSR). For p_T(top) >700 GeV, the peak position is at 400 GeV assuming the same transverse momentum cuts as for low-p_T measurements. This may limit our ability to identify top quarks at such large p_T(top) using the traditional threshold approaches.

Runs at high pileup will also affect other top physics measurements, such as $t(\bar{t})$+jets and associated top production (such as $Ht\bar{t}$), as well as searches for new physics that require a good understanding of low p_T(top) top quarks. Indeed, low-p_T top quarks require the reconstruction of low-p_T(top) jets $(30-100$ GeV), which are exactly the jets that are difficult to correct for pileup effect.

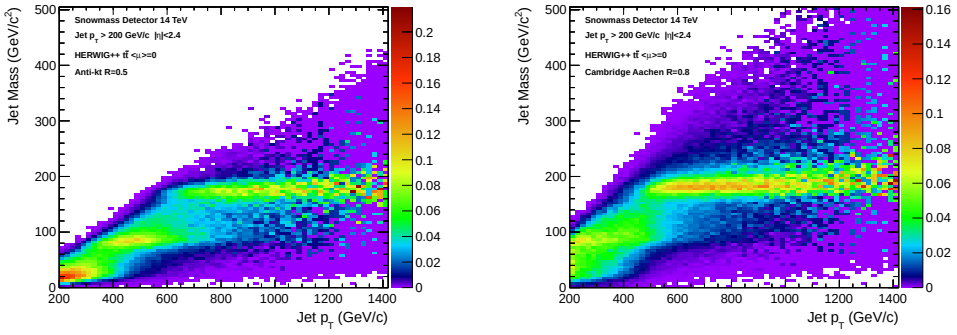

(a) Anti-kt R=0.5

(b) Cambridge Aachen R=0.8

Figure 1-9. *Jet mass vs jet transverse momenta in the* DELPHES *fast simulation for pp collisions at* 14 *TeV for different jet algorithms. The jet transverse spectrum has been reweighed to be flat.*

Perhaps only a combination of multiple measurements by CMS and ATLAS may lead to substantial reduction of systematic detector uncertainties, as the high-luminosity pp collision runs at 14 TeV with $\langle\mu\rangle > 100$ are unfavorable for high precision top quark measurements based on jets with p_T(jet) below 100 GeV. This will also affect searches for new physics that require detection of low-p_T(top) jets. It is therefore crucial to investigate the future of the boosted regime, where different reconstruction techniques can be utilized.

1.7.2 Boosted Top Quarks

The higher energies and luminosities of future LHC upgrades will produce events with a larger number of pileup events, leading to the degradation of precision measurements and searches involving top quark reconstruction. We find that current algorithms for top quark identification at high-p_T can give comparable performance to current conditions, with some modifications to their reconstruction method, or the introduction of detector upgrades.

The decay products of a top quark which is produced at large p_T are sufficiently collimated to be reconstructed within a single jet. This happens above ~ 400 GeV for jets with $R = 0.8$. Figure 1-9 shows the evolution of jet mass with the jet transverse momenta for the $t\bar{t}$ process.

Because all the decay products of a boosted top quark fall within a single jet, specialized techniques involving jet substructure are required. Semileptonic decay reconstructions must introduce modified isolation criteria when the lepton begins to overlap with the additional jet produced in the top quark decay.

The mass of the single jet itself can be a good discriminant between boosted top quarks from and the overwhelming background due to QCD jet production. For example, a recent study [148] has shown that a signal of boosted hadronic top quarks can be observed in the jet mass distribution alone, including jets with $p_T > 800$ GeV/c in the fiducial region of the detector. The jet mass distribution can then be used to set an upper limit on cross sections predicted by certain models. Discrimination can possibly be improved further with the addition of b-tagging.

Jet Grooming. Several algorithms, collectively known as jet grooming algorithms, attempt to mitigate the effect of pileup on jet observables, such as jet mass, by removing soft and wide-angle constituents of jets. The effect of three different jet grooming algorithms have been studied: pruning [149, 150], trimming [151], and filtering [152].

The jet mass distribution can be severely affected by pileup events. For example, the top quark jet mass distribution with 140 additional pileup events is severely shifted and smeared, with a width of more than 50 GeV.

We have found that applying the jet trimming algorithm results in a trimmed jet mass distribution that is relatively stable as the number of pileup events increases. The top quark mass peak is sharpened, having a width of only ~ 15 GeV with 140 added pileup events. Additionally, the jet grooming procedures significantly reduce the masses of QCD jets, enhancing signal discrimination significantly.

Substructure and jet shapes. Jet substructure and jet shapes are often discussed as a useful tool for the identification of top quarks and for reduction of the overwhelming rate from conventional QCD processes [153, 154, 155, 156, 157, 158, 159, 160, 150, 161, 162, 121, 163, 164, 165]. For example, the N-subjettiness algorithm [166] aims to determine the consistency of a jet with a hypothesized number of subjets. Such tools can give good discrimination between top quark jets and QCD jets, however, such discrimination degrades somewhat with the additional pileup activity.

It can also be beneficial to identify the two subjets corresponding to the W boson produced by the top quark decay. Using trimming, a W mass peak can be extracted which is relatively stable even with 140 additional pileup events added. It is advantageous to use one of the jet grooming algorithms, to make the jet mass and other observable quantities less susceptible to pileup activity.

Top Tagging. In addition to the substructure quantities described above, there are several algorithms (top taggers) which attempt to use several quantities in combination to provide additional discrimination.

Two top-tagging algorithms which are currently in use by experimental efforts include the CMS Top Tagger [162] and the HEP Top Tagger [167]. The CMS top tagger is based on an algorithm developed at Johns Hopkins University [158] and decomposes a jet into up to 4 subjets Then, requirements on the jet mass ($140 < m_j < 250$ GeV, number of subjets (3 or more) and a quantity which is a proxy for the mass of the W boson within the jet (minimum pairwise subjet mass > 50 GeV) , are imposed to isolate boosted top quarks. We have studied the effect of pileup on the efficiency of the CMS top tagger. With no additional pileup events, the efficiency of the algorithm maintains its maximum value of $\sim 40\%$ up to jet p_T values of 1.2-1.3 TeV, at which point the efficiency begins to fall to 10% or lower for jets with $p_T > 1.5$ TeV. With additional pileup events (and no correction applied to the subjets), the efficiency degradation happens at much lower p_T values. The rate of QCD jets passing the algorithm is also affected. With no additional pileup events, this mistag rate remains below 5% over the entire range of jet p_T. After adding 140 pileup interactions to the simulated events, the mistag rate from QCD jets increases to a maximum of 45% at a p_T of 500 GeV. A possible tagger was studied, consisting of a trimmed mass cut ($150 < m_j < 230$) and a cut on the number of subjets (≥ 3). This alternative algorithm keeps the mistag rate low (less than $\sim 10\%$), and maintains a high efficiency for top quark identification.

Detector Effects. At extreme values of the top quark p_T, one must begin to consider detector effects. In this regime, top quarks will have hard radiations that may be identified as subjets. Top quark decay products may be so highly collimated that they cannot be individually resolved due to calorimeter detector segmentation and tracking failures.

The effects mentioned above cause a degradation in the top quark jet resolution at large p_T. For example, the width of the top quark jet mass peak increases by a factor of two when comparing top quarks with

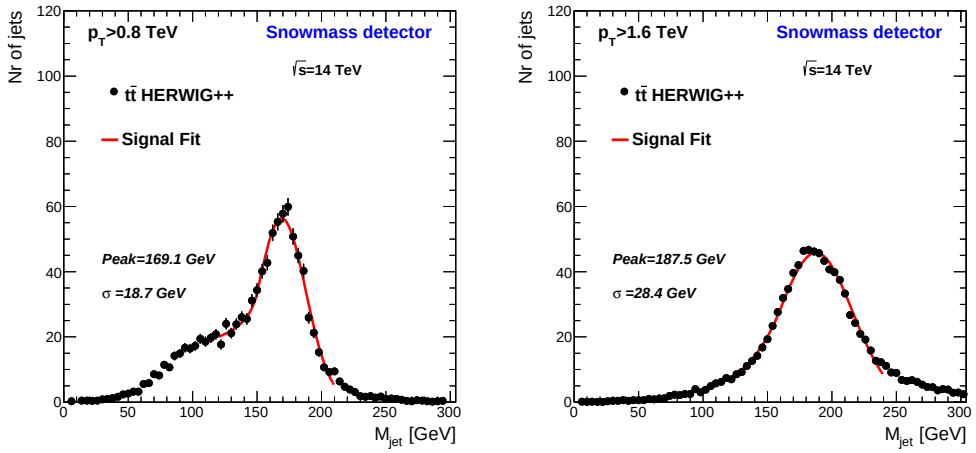

(a) $p_T(jet) > 0.8$ TeV (b) $p_T(jet) > 1.6$ TeV

Figure 1-10. *Jet masses for $t\bar{t}$ events for different p_T(jet) and $\langle\mu\rangle = 140$. The core of the peak was fitted using a Crystal Ball function [168]. All histograms have arbitrary normalization (1000 events).*

$p_T > 1.6$ TeV to those with $p_T > 0.8$ TeV, see Fig. 1-10. The effect of a shrinking jet distance parameter, $R \sim 1/p_T$, improves the resolution of the top quark jet mass peak at high-p_T, by removing additional hard radiations from the top quark.

Finally, it can be beneficial to increase the granularity of individual calorimeter cells used in event reconstruction, which provides and increased top quark jet mass resolution.

1.7.3 Linear Colliders

A linear collider e^+e^- will allow for studying electroweak production of $t\bar{t}$ pairs with no concurring QCD background. Linear colliders can use polarized beams, giving samples enriched in top quarks of left or right handed helicities. This can allow one to probe new physics scenarios predicting anomalous production rates of right-handed t quarks compared to the SM.

Due to the electroweak production mechanism, all interesting processes occur at roughly the same rate, and backgrounds can be reduced to a negligible level. After applying selection cuts, it is possible to retain a signal sample of approximately 10^5 events. Unlike at the LHC, there are no or few additional interactions (pileup) per beam crossing, especially for the ILC. Additional activity may come from $\gamma\gamma$ interactions. Ongoing studies show that this residual pile-up can be controlled when applying the invariant k_t jet algorithm [169, 170] for background suppression.

The top quark mass can be measured in two ways. First, using the invariant mass of the reconstructed bW system from the top decay. The result of a full simulation study at a centre of mass energy of 500 GeV [6] is shown in Fig. 1-11. The figure demonstrates also the small residual background expected for top quark studies at e^+e^- machines. In the second method the top mass is determined in a threshold scan, an option unique to an e^+e^- machine. In the threshold scan the top mass can be measured to a precision of better

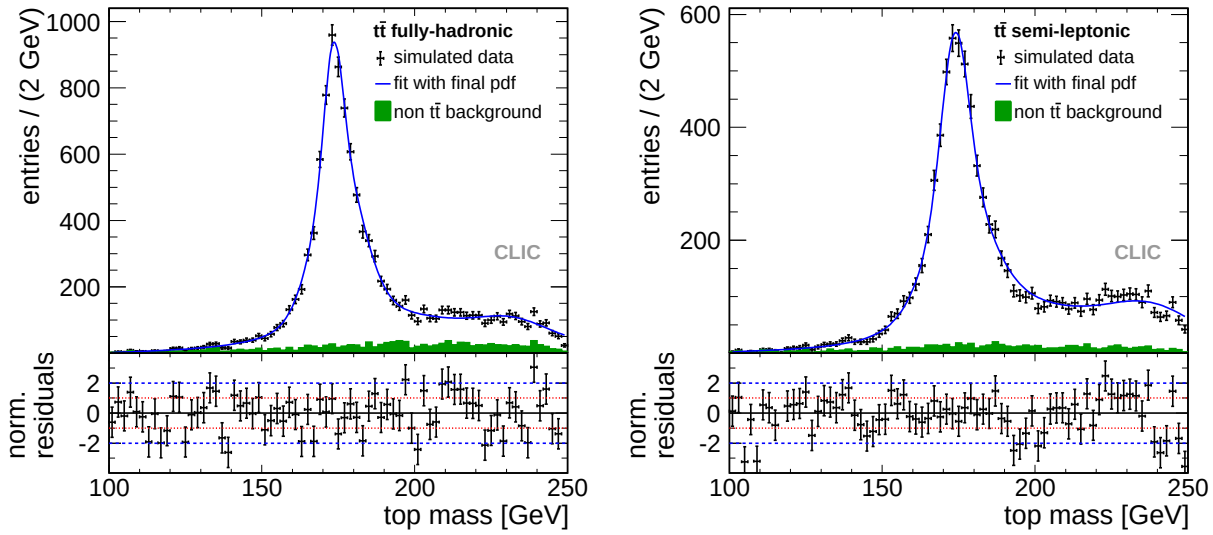

Figure 1-11. *Distribution of reconstructed top mass for events classified as fully-hadronic (left) and semi-leptonic (right). The data points include signal and background for an integrated luminosity of 100 fb^{-1}. The pure background contribution contained in the global distribution is shown by the green solid histogram. The top mass is determined with an unbinned likelihood fit of this distribution, which is shown by the solid line.*

than 40 MeV where systematic studies have shown that the statistical error is dominant. However, using the $\overline{\text{MS}}$ mass will inflate the uncertainty to ~ 100 MeV.

Observables such as A^t_{FB} or the slope of the helicity angle λ_t [171] are sensitive to the chiral structure of the $t\bar{t}X$ vertex. A result of a full simulation study of semi-leptonic $t\bar{t}$ decays [172] is shown in Fig. 1-12. It demonstrates that it will be possible to measure both the production angle θ_{top} of the t quark and the helicity angle θ_{hel} to great precision over a large range, leading to measurements of A^t_{FB} and λ_t with a precision of about 2%. Additionally, the A^t_{FB} and other measurements of the $t\bar{t}$ system, will benefit from a $> 60\%$ pure sample [175] in which to measure the b quark charge. The chiral structures of couplings can be possibly be probed in this way.

Using A^t_{FB}, λ_t and the $t\bar{t}$ production cross section, electroweak couplings can be determined at the percent level. It is important that experimental and theoretical errors are kept at the same level. This requires a precise measurement of, for example, the luminosity and the beam polarization. Currently, both parameters are expected to be controlled to better than 0.5%. In general the realization of machine and detectors must not compromise the precision physics. This is maybe the biggest challenge in the coming years.

1.8 Conclusions

(*still under construction*)

The LHC and a future lepton collider provide complementary information on top quark couplings. The LHC will probe the top coupling to the gluon and W boson precisely, while the couplings to the photon and Z boson will be precisely measured at a lepton collider. The top Yukawa coupling will be measured to roughly equal precision at the LHC and a future lepton collider.

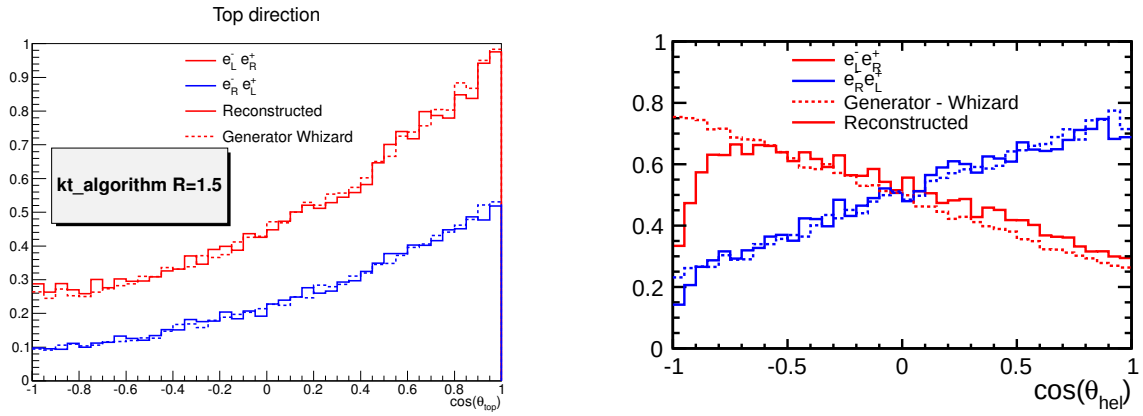

Figure 1-12. *Left: Reconstructed forward backward asymmetry compared with the prediction by the event generator WHIZARD [173, 174]. Right: Polar angle of the decay lepton in the rest frame of the t quark.*

As far as top quark rare decays are concerned, the LHC and a future lepton collider can again be complementary, for example, the LHC is better at probing the associated couplings involving gluon, but it is difficult to probe the spin structure of couplings unlike at a lepton collider.

Given the present bounds on stops, top-partners and resonance decaying into $t\bar{t}$, it seems difficult to produce these particles directly at < 1 TeV lepton collider so that the LHC is the only option here.

References

[1] F. Abe et al. Observation of top quark production in $\bar{p}p$ collisions. *Phys.Rev.Lett.*, 74:2626–2631, 1995.

[2] S. Abachi et al. Observation of the top quark. *Phys.Rev.Lett.*, 74:2632–2637, 1995.

[3] Giuseppe Degrassi, Stefano Di Vita, Joan Elias-Miro, Jose R. Espinosa, Gian F. Giudice, et al. Higgs mass and vacuum stability in the Standard Model at NNLO. *JHEP*, 1208:098, 2012.

[4] M. Baak, M. Goebel, J. Haller, A. Hoecker, D. Kennedy, et al. The Electroweak Fit of the Standard Model after the Discovery of a New Boson at the LHC. *Eur.Phys.J.*, C72:2205, 2012.

[5] Manel Martinez and Ramon Miquel. Multiparameter fits to the t anti-t threshold observables at a future e+ e- linear collider. *Eur.Phys.J.*, C27:49–55, 2003.

[6] Katja Seidel, Frank Simon, Michal Tesar, and Stephane Poss. Top quark mass measurements at and above threshold at CLIC. 2013.

[7] Martin Beneke, Yuichiro Kiyo, and Kurt Schuller. NNNLO results on top-quark pair production near threshold. *PoS*, RADCOR2007:051, 2007.

[8] Serguei Chatrchyan et al. Measurement of the top-quark mass in $t\bar{t}$ events with lepton+jets final states in pp collisions at $\sqrt{s} = 7$ TeV. *JHEP*, 1212:105, 2012.

[9] Serguei Chatrchyan et al. Measurement of masses in the $t\bar{t}$ system by kinematic endpoints in pp collisions at $\sqrt{s}$=7 TeV. 2013.

[10] Avto Kharchilava. Top mass determination in leptonic final states with J/ψ. *Phys.Lett.*, B476:73–78, 2000.

[11] Ansgar Denner, Stefan Dittmaier, Stefan Kallweit, and Stefano Pozzorini. NLO QCD corrections to off-shell top-antitop production with leptonic decays at hadron colliders. *JHEP*, 1210:110, 2012.

[12] Giuseppe Bevilacqua, Michal Czakon, Andreas van Hameren, Costas G. Papadopoulos, and Malgorzata Worek. Complete off-shell effects in top quark pair hadroproduction with leptonic decay at next-to-leading order. *JHEP*, 1102:083, 2011.

[13] ATLAS collaboration. Measurement of the Top Quark Mass from $\sqrt{s} = 7$ TeV ATLAS data using a 3-dimensional template fit. *ATLAS-CONF-2013-046*, 2013.

[14] Sandip Biswas, Kirill Melnikov, and Markus Schulze. Next-to-leading order QCD effects and the top quark mass measurements at the LHC. *JHEP*, 1008:048, 2010.

[15] Simone Alioli, Patricia Fernandez, Juan Fuster, Adrian Irles, Sven-Olaf Moch, et al. A new observable to measure the top-quark mass at hadron colliders. *Eur.Phys.J.*, C73:2438, 2013.

[16] J.A. Aguilar-Saavedra. A Minimal set of top anomalous couplings. *Nucl.Phys.*, B812:181–204, 2009.

[17] Cen Zhang and Scott Willenbrock. Effective Field Theory for Top Quark Physics. *Nuovo Cim.*, C033N4:285–291, 2010.

[18] M Baumgart, A Loginov, A Garcia-Bellido, and J Adelman. Summary of "Top couplings" High Energy Frontier Study Group. 2013.

[19] Nicola Cabibbo. Unitary Symmetry and Leptonic Decays. *Phys.Rev.Lett.*, 10:531–533, 1963.

[20] H. Lacker, A. Menzel, F. Spettel, D. Hirschbuhl, J. Luck, et al. Model-independent extraction of $|V_{tq}|$ matrix elements from top-quark measurements at hadron colliders. *Eur.Phys.J.*, C72:2048, 2012.

[21] Georges Aad et al. Measurement of the t-channel single top-quark production cross section in pp collisions at $\sqrt{s} = 7$ TeV with the ATLAS detector. *Phys.Lett.*, B717:330–350, 2012.

[22] Serguei Chatrchyan et al. Measurement of the single-top-quark t-channel cross section in pp collisions at $\sqrt{s} = 7$ TeV. *JHEP*, 1212:035, 2012.

[23] Georges Aad et al. Evidence for the associated production of a W boson and a top quark in ATLAS at $\sqrt{s} = 7$ TeV. *Phys.Lett.*, B716:142–159, 2012.

[24] Search for $\mathcal{CP}$ violation in single top quark events in pp collisions at $\sqrt{s} = 7$ tev with the atlas detector. Technical Report ATLAS-CONF-2013-032, 2013.

[25] E. Boos, M. Dubinin, A. Pukhov, M. Sachwitz, and H.J. Schreiber. Single top production in e+ e-, e- e-, gamma e and gamma gamma collisions. *Eur.Phys.J.*, C21:81–91, 2001.

[26] Sukanta Dutta, Ashok Goyal, Mukesh Kumar, and Bruce Mellado. Measuring anomalous Wtb couplings at $e^- p$ collider. 2013.

[27] A. Juste, Y. Kiyo, F. Petriello, T. Teubner, K. Agashe, et al. Report of the 2005 Snowmass top/QCD working group. 2006.

[28] Howard Baer, Tim Barklow, Keisuke Fujii, Yuanning Gao, Andre Hoang, et al. The International Linear Collider Technical Design Report - Volume 2: Physics. 2013.

[29] Cms at the high-energy frontier. contribution to the update of the european strategy for particle physics. Technical Report CMS-NOTE-2012-006. CERN-CMS-NOTE-2012-006, CERN, Geneva, Oct 2012.

[30] The ATLAS-collaboration. Physics at a high-luminosity lhc with atlas (update). Technical Report ATL-PHYS-PUB-2012-004, CERN, Geneva, Oct 2012.

[31] Arnaud Gay. Measurement of the top-Higgs Yukawa coupling at a Linear e+ e- Collider. *Eur.Phys.J.*, C49:489–497, 2007.

[32] J. Shelton A. Jung, M. Schulze. Kinematics of Top Quark Final States. *Snowmass 2013 whitepaper, in preparation.*

[33] John M. Campbell and R.K. Ellis. MCFM for the Tevatron and the LHC. *Nucl.Phys.Proc.Suppl.*, 205-206:10–15, 2010.

[34] Leandro G. Almeida, George Sterman, and Werner Vogelsang. Threshold resummation for the top quark charge asymmetry. *Phys. Rev. D*, 78:014008, Jul 2008.

[35] Oscar Antuñano, Johann H. Kühn, and Germán Rodrigo. Top quarks, axigluons, and charge asymmetries at hadron colliders. *Phys. Rev. D*, 77:014003, Jan 2008.

[36] M. T. Bowen, S. D. Ellis, and D. Rainwater. Standard model top quark asymmetry at the fermilab tevatron. *Phys. Rev. D*, 73:014008, Jan 2006.

[37] CDF Collaboration. Measurement of the top quark forward-backward production asymmetry and its dependence on event kinematic properties. *Phys. Rev. D*, 87:092002, May 2013.

[38] D0 Collaboration. Measurement of leptonic asymmetries and top-quark polarization in $t\bar{t}$ production. *Phys. Rev. D*, 87:011103, Jan 2013.

[39] ATLAS Collaboration. Measurement of the charge asymmetry in top quark pair production in pp collisions at $\sqrt{s} = 7$ TeV using the ATLAS detector. *Eur.Phys.J.*, C72:2039, 2012.

[40] CMS Collaboration. Measurement of the charge asymmetry in top-quark pair production in protonproton collisions at. *Physics Letters B*, 709(12):28 – 49, 2012.

[41] Werner Bernreuther and Zong-Guo Si. Top quark and leptonic charge asymmetries for the tevatron and lhc. *Phys. Rev. D*, 86:034026, Aug 2012.

[42] Measurement of the charge asymmetry in dileptonic decay of top quark pairs in pp collisions at s = 7 tev using the atlas detector. Technical Report ATLAS-CONF-2012-057, CERN, Geneva, Jun 2012.

[43] Top charge asymmetry measurement in dileptons at 7 tev. Technical Report CMS-PAS-TOP-12-010, CERN, Geneva, 2012.

[44] Werner Bernreuther and Zong-Guo Si. Top quark and leptonic charge asymmetries for the Tevatron and LHC. *Phys.Rev.*, D86:034026, 2012.

[45] Paul H. Frampton, Jing Shu, and Kai Wang. Axigluon as Possible Explanation for p anti-p -¿ t anti-t Forward-Backward Asymmetry. *Phys.Lett.*, B683:294–297, 2010.

[46] Yang Bai, JoAnne L. Hewett, Jared Kaplan, and Thomas G. Rizzo. LHC Predictions from a Tevatron Anomaly in the Top Quark Forward-Backward Asymmetry. *JHEP*, 1103:003, 2011.

[47] Gustavo Marques Tavares and Martin Schmaltz. Explaining the t-tbar asymmetry with a light axigluon. *Phys.Rev.*, D84:054008, 2011.

[48] Moira Gresham, Jessie Shelton, and Kathryn M. Zurek. Open windows for a light axigluon explanation of the top forward-backward asymmetry. *JHEP*, 1303:008, 2013.

[49] Ulrich Haisch and Susanne Westhoff. Massive Color-Octet Bosons: Bounds on Effects in Top-Quark Pair Production. *JHEP*, 1108:088, 2011.

[50] R. Sekhar Chivukula, Elizabeth H. Simmons, and C.-P. Yuan. Axigluons cannot explain the observed top quark forward-backward asymmetry. *Phys.Rev.*, D82:094009, 2010.

[51] Mirjam Cvetic, James Halverson, and Paul Langacker. Ultraviolet Completions of Axigluon Models and Their Phenomenological Consequences. *JHEP*, 1211:064, 2012.

[52] S. Dittmaier, P. Uwer, and S. Weinzierl. Hadronic top-quark pair production in association with a hard jet at next-to-leading order QCD: Phenomenological studies for the Tevatron and the LHC. *Eur. Phys. J.*, C59:625–646, 2009.

[53] Kirill Melnikov and Markus Schulze. NLO QCD corrections to top quark pair production in association with one hard jet at hadron colliders. *Nucl.Phys.*, B840:129–159, 2010.

[54] Stefan Berge and Susanne Westhoff. Top-Quark Charge Asymmetry Goes Forward: Two New Observables for Hadron Colliders. 2013.

[55] Stefan Berge and Susanne Westhoff. Charge Asymmetry in Top Pair plus Jet Production A Snowmass White Paper . *Snowmass 2013 whitepaper, in preparation.*

[56] Alexander L. Kagan, Jernej F. Kamenik, Gilad Perez, and Sheldon Stone. Top LHCb Physics. *Phys.Rev.Lett.*, 107:082003, 2011.

[57] Victor Mukhamedovich Abazov et al. Evidence for spin correlation in $t\bar{t}$ production. *Phys.Rev.Lett.*, 108:032004, 2012.

[58] ATLAS Collaboration. Observation of spin correlation in $t\bar{t}$ events from pp collisions at sqrt(s) = 7 TeV using the ATLAS detector. *Phys.Rev.Lett.*, 108:212001, 2012.

[59] Measurement of spin correlations in ttbar production. Technical Report CMS-PAS-TOP-12-004, CERN, Geneva, 2012.

[60] Kirill Melnikov and Markus Schulze. NLO QCD corrections to top quark pair production and decay at hadron colliders. *JHEP*, 0908:049, 2009.

[61] Werner Bernreuther and Zong-Guo Si. Distributions and correlations for top quark pair production and decay at the Tevatron and LHC. *Nucl.Phys.*, B837:90–121, 2010.

[62] Matthew Baumgart and Brock Tweedie. Discriminating Top-Antitop Resonances using Azimuthal Decay Correlations. *JHEP*, 1109:049, 2011.

[63] Fabrizio Caola, Kirill Melnikov, and Markus Schulze. A complete next-to-leading order QCD description of resonant Z' production and decay into $t\bar{t}$ final states. *Phys.Rev.*, D87:034015, 2013.

[64] Matthew Baumgart and Brock Tweedie. A New Twist on Top Quark Spin Correlations. *JHEP*, 1303:117, 2013.

[65] Werner Bernreuther and Zong-Guo Si. Top quark spin correlations and polarization at the LHC: standard model predictions and effects of anomalous top chromo moments. 2013.

[66] N. Craig and M. Velasco. Top Rare Decays. *Snowmass whitepaper, in preparation.*

[67] J.A. Aguilar-Saavedra. Top flavor-changing neutral interactions: Theoretical expectations and experimental detection. *Acta Phys.Polon.*, B35:2695–2710, 2004.

[68] David Atwood, Laura Reina, and Amarjit Soni. Phenomenology of two Higgs doublet models with flavor changing neutral currents. *Phys.Rev.*, D55:3156–3176, 1997.

[69] Santi Bejar. Flavor changing neutral decay effects in models with two Higgs boson doublets: Applications to LHC Physics. 2006.

[70] J.J. Cao, G. Eilam, M. Frank, K. Hikasa, G.L. Liu, et al. SUSY-induced FCNC top-quark processes at the large hadron collider. *Phys.Rev.*, D75:075021, 2007.

[71] Jin Min Yang, Bing-Lin Young, and X. Zhang. Flavor changing top quark decays in r parity violating SUSY. *Phys.Rev.*, D58:055001, 1998.

[72] G. Eilam, A. Gemintern, Tao Han, J.M. Yang, and X. Zhang. Top quark rare decay $t \to ch$ in R-parity violating SUSY. *Phys.Lett.*, B510:227–235, 2001.

[73] Kaustubh Agashe, Gilad Perez, and Amarjit Soni. Collider Signals of Top Quark Flavor Violation from a Warped Extra Dimension. *Phys.Rev.*, D75:015002, 2007.

[74] Kaustubh Agashe and Roberto Contino. Composite Higgs-Mediated FCNC. *Phys.Rev.*, D80:075016, 2009.

[75] G. Eilam, J.L. Hewett, and A. Soni. Rare decays of the top quark in the standard and two Higgs doublet models. *Phys.Rev.*, D44:1473–1484, 1991.

[76] B. Mele, S. Petrarca, and A. Soddu. A New evaluation of the t-¿cH decay width in the standard model. *Phys.Lett.*, B435:401–406, 1998.

[77] Michael E. Luke and Martin J. Savage. Flavor changing neutral currents in the Higgs sector and rare top decays. *Phys.Lett.*, B307:387–393, 1993.

[78] Serguei Chatrchyan et al. Search for flavor changing neutral currents in top quark decays in pp collisions at 7 TeV. *Phys.Lett.*, B718:1252–1272, 2013.

[79] Georges Aad et al. Search for FCNC single top-quark production at $\sqrt{s} = 7$ TeV with the ATLAS detector. *Phys.Lett.*, B712:351–369, 2012.

[80] F. Abe et al. Search for flavor-changing neutral current decays of the top quark in $p\bar{p}$ collisions at $\sqrt{s} = 1.8$ TeV. *Phys.Rev.Lett.*, 80:2525–2530, 1998.

[81] F. et al. [CDF Collaboration] Abe. . *CDF/PUB/TOP/PUBLIC/9496.*

[82] F.D. Aaron et al. Search for Single Top Quark Production at HERA. *Phys.Lett.*, B678:450–458, 2009.

[83] Nathaniel Craig, Jared A. Evans, Richard Gray, Michael Park, Sunil Somalwar, et al. Searching for $t \to ch$ with Multi-Leptons. *Phys.Rev.*, D86:075002, 2012.

[84] Georges Aad et al. A search for flavour changing neutral currents in top-quark decays in pp collision data collected with the ATLAS detector at $\sqrt{s} = 7$ TeV. *JHEP*, 1209:139, 2012.

[85] Patrick J. Fox, Zoltan Ligeti, Michele Papucci, Gilad Perez, and Matthew D. Schwartz. Deciphering top flavor violation at the LHC with B factories. *Phys.Rev.*, D78:054008, 2008.

[86] Roni Harnik, Joachim Kopp, and Jure Zupan. Flavor Violating Higgs Decays. *JHEP*, 1303:026, 2013.

[87] ATLAS-Collaboration. Physics at a High-Luminosity LHC with ATLAS. *ATL-PHYS-PUB-2012-001.*

[88] N. Craig. . *private communication.*

[89] Jun Gao, Chong Sheng Li, Li Lin Yang, and Hao Zhang. Search for anomalous top quark production at the early LHC. *Phys.Rev.Lett.*, 107:092002, 2011.

[90] J.A. Aguilar-Saavedra and T. Riemann. Probing top flavor changing neutral couplings at TESLA. 2001.

[91] Tao Han and JoAnne L. Hewett. Top charm associated production in high-energy e^+e^- collisions. *Phys.Rev.*, D60:074015, 1999.

[92] ATLAS Collaboration. Search for direct production of the top squark in the all-hadronic ttbar + etmiss final state in 21 fb-1 of p-pcollisions at sqrt(s)=8 TeV with the ATLAS detector. *ATLAS-CONF-2013-024.*

[93] CMS Collaboration. Search for top-squark pair production in the single lepton final state in pp collisions at 8 TeV. *CMS-PAS-SUS-13-011.*

[94] ATLAS Collaboration. Searches for Supersymmetry at the high luminosity LHC with the ATLAS Detector. *ATL-PHYS-PUB-2013-002. [European strategy study; update with their Snowmass white paper when available].*

[95] Jim Olson. . *talk at the Seattle energy frontier workshop [replace with CMS white paper reference when available].*

[96] Z Ha and A Katz. Stealth Stops. *Snowmass white paper, in preparation.*

[97] Zhenyu Han, Andrey Katz, David Krohn, and Matthew Reece. (Light) Stop Signs. *JHEP*, 1208:083, 2012.

[98] Can Kilic and Brock Tweedie. Cornering Light Stops with Dileptonic mT2. *JHEP*, 1304:110, 2013.

[99] A. G. et al. Delannoy. Probing Stealthy, Compressed, and Light Stops with Vector Boson Fusion at the LHC. *Snowmass white paper, in preparation.*

[100] Christopher Brust, Andrey Katz, Scott Lawrence, and Raman Sundrum. SUSY, the Third Generation and the LHC. *JHEP*, 1203:103, 2012.

[101] ATLAS Collaboration. Search for strong production of supersymmetric particles in final states with missing transverse momentum and at least three b-jets using 20.1 fb^{-1} of pp collisions at sqrt(s) = 8 TeV with the ATLAS Detector. *ATLAS-CONF-2013-061.*

[102] CMS Collaboration. Search for Supersymmetry in pp collisions at 8 TeV in events with a single lepton, multiple jets and b-tags. *CMS-PAS-SUS-13-007.*

[103] S. et al. Chekanov. Detectors and algorithms. *Section 1.7 of this report.*

[104] Joshua Berger, Maxim Perelstein, Michael Saelim, and Andrew Spray. Boosted Tops from Gluino Decays. 2011.

[105] M. Graesser. Asymmetric Stop Decays and Topness at the 14 TeV LHC. *Snowmass white paper, in preparation.*

[106] Michael L. Graesser and Jessie Shelton. Hunting Asymmetric Stops. 2012.

[107] B. et al. Dutta. Top Squark Searches and Well-Tempered Bino/Higgsino Dark Matter at the LHC. *Snowmass white paper, in preparation.*

[108] N. Arkani-Hamed, A. Delgado, and G.F. Giudice. The Well-tempered neutralino. *Nucl.Phys.*, B741:108–130, 2006.

[109] Emanuel Nikolidakis and Christopher Smith. Minimal Flavor Violation, Seesaw, and R-parity. *Phys.Rev.*, D77:015021, 2008.

[110] Csaba Csaki, Yuval Grossman, and Ben Heidenreich. MFV SUSY: A Natural Theory for R-Parity Violation. *Phys.Rev.*, D85:095009, 2012.

[111] Joshua Berger, Maxim Perelstein, Michael Saelim, and Philip Tanedo. The Same-Sign Dilepton Signature of RPV/MFV SUSY. *JHEP*, 1304:077, 2013.

[112] Zhenyu Han, Andrey Katz, Minho Son, and Brock Tweedie. Boosting Searches for Natural SUSY with RPV via Gluino Cascades. 2012.

[113] A. Katz. Search for RPV Gluino in RPV Natural SUSY. *Snowmass white paper, in preparation.*

[114] S. Bhattacharya, U. Heintz, and M. Narain. Prospects for Heavy Vector-like Charge 2/3 Quarks at the LHC with $\sqrt{s} = 14$ and 33 TeV. *Snowmass white paper, in preparation.*

[115] T. Andeen, K. Black, C. Bernard, T. Childress, L. Dell'Asta, and N. Vignaroli. Prospects for Single Production of Vector-Like Quarks at 14 and 33 TeV. *Snowmass white paper, in preparation.*

[116] E. Varnes. Potential of future accelerators for observing vector-like bottom-partner pair production. *Snowmass white paper, in preparation.*

[117] T. Avetisyan, A. and Bose. Search for top partners with charge $5e/3$. *Snowmass white paper, in preparation.*

[118] Robert M. Harris, Christopher T. Hill, and Stephen J. Parke. Cross-section for topcolor Z-prime(t) decaying to t anti-t: Version 2.6. 1999.

[119] Lisa Randall and Raman Sundrum. A Large mass hierarchy from a small extra dimension. *Phys.Rev.Lett.*, 83:3370–3373, 1999.

[120] A. Effron, J. Erdmann, T. Golling, and C. Pollard. Search for $t\bar{t}$ resonances at future hadron colliders for Snowmass 2013. *Snowmass white paper, in preparation.*

[121] Leandro G. Almeida, Seung J. Lee, Gilad Perez, George Sterman, and Ilmo Sung. Template Overlap Method for Massive Jets. *Phys.Rev.*, D82:054034, 2010.

[122] Mihailo Backovic, Jose Juknevich, and Gilad Perez. Boosting the Standard Model Higgs Signal with the Template Overlap Method. 2012.

[123] Georges Aad et al. Search for resonances decaying into top-quark pairs using fully hadronic decays in pp collisions with ATLAS at $\sqrt{s} = 7$ TeV. *JHEP*, 1301:116, 2013.

[124] M. Backovic and S. J. Lee. Searches for RS KK-gluons with the Template Overlap Method in the high end of boosted top regime. *Snowmass white paper, in preparation.*

[125] G. Aad et al. The atlas experiment at the cern large hadron collider. *JINST*, 3:S08003, 2008.

[126] S Chatrchyan et al. The cms experiment at the cern lhc. *Journal of Instrumentation*, 3(08):S08004, 2008.

[127] Georges Aad et al. Measurement of the top quark-pair production cross section with ATLAS in pp collisions at $\sqrt{s} = 7$ TeV. *Eur.Phys.J.*, C71:1577, 2011.

[128] G. Aad et al. Measurement of the top quark pair production cross section in pp collisions at $\sqrt{s} = 7$ TeV in dilepton final states with ATLAS. *Phys. Lett.*, B707:459–477, 2012.

[129] G. Aad et al. Measurement of the top quark pair production cross-section with ATLAS in the single lepton channel. *Phys.Lett.*, B711:244–263, 2012.

[130] G. Aad et al. Measurement of the cross section for top-quark pair production in pp collisions at $\sqrt{s} = 7$ TeV with the ATLAS detector using final states with two high-pt leptons. *JHEP*, 1205:059, 2012.

[131] G. Aad et al. Measurement of the top quark pair cross section with ATLAS in pp collisions at sqrt(s) = 7 TeV using final states with an electron or a muon and a hadronically decaying τ lepton. *Phys.Lett.*, B717:89–108, 2012.

[132] G. Aad et al. Measurements of top quark pair relative differential cross-sections with ATLAS in pp collisions at $\sqrt{s} = 7$ TeV. *Eur.Phys.J.*, C73:2261, 2013.

[133] S. Chatrchyan et al. Measurement of the t-channel single top quark production cross section in pp collisions at $\sqrt{s} = 7$ tev. *Phys. Rev. Lett.*, 107(arXiv:1106.3052. CMS-TOP-10-008. CERN-PH-EP-2011-066):091802. 27 p, Jun 2011.

[134] S. Chatrchyan et al. Measurement of the $t\bar{t}$ production cross section in the dilepton channel in pp collisions at $\sqrt{s}$=7 tev. *J. High Energy Phys.*, 11(arXiv:1208.2671. CMS-TOP-11-005. CERN-PH-EP-2012-224):067. 39 p, Aug 2012.

[135] S. Chatrchyan et al. Measurement of the $t\bar{t}$ production cross section in pp collisions at $\sqrt{s}$ = 7 tev with lepton + jets final states. *Phys. Lett. B*, 720(arXiv:1212.6682. CMS-TOP-11-003. CERN-PH-EP-2012-285):83. 31 p, Dec 2012.

[136] G. Aad et al. Measurement of the top quark mass with the template method in the $t\bar{t}$ lepton + jets channel using ATLAS data. *Eur.Phys.J.*, C72:2046, 2012.

[137] S. Chatrchyan et al. Measurement of the top-quark mass in $t\bar{t}$ events with dilepton final states in pp collisions at $\sqrt{s}$=7 tev. *Eur. Phys. J. C*, 72(arXiv:1209.2393. CMS-TOP-11-016. CERN-PH-EP-2012-222):2202, Sep 2012.

[138] S. Chatrchyan et al. Measurement of the $t\bar{t}$ production cross section and the top quark mass in the dilepton channel in pp collisions at $\sqrt{s}$ =7 tev. *J. High Energy Phys.*, 07(arXiv:1105.5661. CMS-TOP-11-002. CERN-PH-EP-2011-055):049. 44 p, May 2011.

[139] S. Chatrchyan et al. Measurement of the single-top-quark t-channel cross section in pp collisions at $\sqrt{s}$ = 7 tev. *J. High Energy Phys.*, 12(arXiv:1209.4533. CMS-TOP-11-021. CERN-PH-EP-2012-274):035. 41 p, Sep 2012.

[140] R. Calkins, Chekanov S., Dolen J., Pilot J., Pöschl R., and Tweedie. B. Reconstructing top quarks at the upgraded LHC and at future accelerators. Summary of "Top algorithms and detectors" High Energy Frontier Study Group. 2013.

[141] Torbjorn Sjostrand, Stephen Mrenna, and Peter Z. Skands. PYTHIA 6.4 Physics and Manual. *JHEP*, 05:026, 2006.

[142] M Bahr et al. Herwig++ physics and manual. 2008. Herwig++ Physics and Manual.

[143] S. Ovyn, X. Rouby, and V. Lemaitre. DELPHES, a framework for fast simulation of a generic collider experiment. Technical report, 2009.

[144] Snowmass2013 MC simulation group. Delphes simulation samples for the top-quark group. Snowmass Wiki, 2013. http://www.snowmass2013.org/tiki-index.php?page=SimulationSamples.

[145] Matteo Cacciari, Gavin P. Salam, and Gregory Soyez. FastJet User Manual. *Eur. Phys. J.*, C72:1896, 2012.

[146] Matteo Cacciari, Gavin P. Salam, and Gregory Soyez. The anti-k_t jet clustering algorithm. *JHEP*, 04:063, 2008.

[147] Measurement of the top quark mass from 2011 atlas data using the template method. Technical Report ATLAS-CONF-2011-120, CERN, Geneva, Aug 2011.

[148] B. Auerbach, S.V. Chekanov, and N. Kidonakis. Studies of highly-boosted top quarks near the TeV scale using jet masses at the LHC. 2013. arXiv:1301.5810. Also as SNOW13-00027.

[149] Stephen D. Ellis, Christopher K. Vermilion, and Jonathan R. Walsh. Recombination Algorithms and Jet Substructure: Pruning as a Tool for Heavy Particle Searches. 2009.

[150] Stephen D. Ellis, Christopher K. Vermilion, and Jonathan R. Walsh. Techniques for improved heavy particle searches with jet substructure. *Phys. Rev.*, D 80:051501, 2009.

[151] David Krohn, Jesse Thaler, and Lian-Tao Wang. Jet Trimming. *JHEP*, 1002:084, 2010.

[152] Jonathan M. Butterworth, Adam R. Davison, Mathieu Rubin, and Gavin P. Salam. Jet substructure as a new higgs search channel at the lhc. *Phys. Rev. Lett.*, 100:242001, 2008.

[153] Kaustubh Agashe, Alexander Belyaev, Tadas Krupovnickas, Gilad Perez, and Joseph Virzi. LHC signals from warped extra dimensions. *Phys. Rev.*, D77:015003, 2008.

[154] Ben Lillie, Lisa Randall, and Lian-Tao Wang. The Bulk RS KK-gluon at the LHC. *JHEP*, 09:074, 2007.

[155] J. M. Butterworth, John R. Ellis, and A. R. Raklev. Reconstructing sparticle mass spectra using hadronic decays. *JHEP*, 05:033, 2007.

[156] Leandro G. Almeida, Seung J. Lee, Gilad Perez, Ilmo Sung, and Joseph Virzi. Top Jets at the LHC. *Phys. Rev.*, D 79:074012, 2009.

[157] Leandro G. Almeida et al. Substructure of high-p_T Jets at the LHC. *Phys. Rev.*, D 79:074017, 2009.

[158] David E. Kaplan, Keith Rehermann, Matthew D. Schwartz, and Brock Tweedie. Top Tagging: A Method for Identifying Boosted Hadronically Decaying Top Quarks. *Phys. Rev. Lett.*, 101:142001, 2008.

[159] Gustaaf H Brooijmans. High pT Hadronic Top Quark Identification. Published in "A Les Houches Report. Physics at Tev Colliders 2007 – New Physics Working Group", 2008.

[160] Jonathan M. Butterworth et al. Discovering baryon-number violating neutralino decays at the LHC. Technical Report CERN-PH-TH/2009-073, hep-ph/0906.0728, 2009.

[161] Reconstruction of high mass $t\bar{t}$ resonances in the lepton+jets channel. Technical Report ATL-PHYS-PUB-2009-081. ATL-COM-PHYS-2009-255, CERN, Geneva, May 2009.

[162] A cambridge-aachen (c-a) based jet algorithm for boosted top-jet tagging. Technical Report CMS-PAS-JME-09-001, Jul 2009.

[163] Christoph Hackstein and Michael Spannowsky. Boosting Higgs discovery - the forgotten channel, 2010, hep-ph:1008.2202.

[164] S. Chekanov and J. Proudfoot. Searches for TeV-scale particles at the LHC using jet shapes. *Phys. Rev.*, D81:114038, 2010.

[165] S. V. Chekanov, C. Levy, J. Proudfoot, and R. Yoshida. New approach for jet-shape identification of TeV-scale particles at the LHC. *Phys. Rev.*, D82:094029, 2010.

[166] Jesse Thaler and Ken Tilburg. Identifying boosted objects with n-subjettiness. *Journal of High Energy Physics*, 2011(3):1–28, 2011.

[167] Tilman Plehn, Michael Spannowsky, Michihisa Takeuchi, and Dirk Zerwas. Stop Reconstruction with Tagged Tops. *JHEP*, 1010:078, 2010.

[168] M.J. Oreglia. A Study of the Reactions psi prime to gamma gamma psi,. Ph.D. Thesis, SLAC-R-236, 1980.

[169] S. Catani, Yuri L. Dokshitzer, M. H. Seymour, and B. R. Webber. Longitudinally invariant K_t clustering algorithms for hadron hadron collisions. *Nucl. Phys.*, B406:187–224, 1993.

[170] Stephen D. Ellis and Davison E. Soper. Successive combination jet algorithm for hadron collisions. *Phys. Rev.*, D48:3160–3166, 1993.

[171] Edmond L. Berger, Qing-Hong Cao, Chuan-Ren Chen, Jiang-Hao Yu, and Hao Zhang. The Top Quark Production Asymmetries A_{FB}^t and A_{FB}^ℓ. *Phys.Rev.Lett.*, 108:072002, 2012.

[172] M.S. Amjad et al. A precise determination of top quark electroweak couplings at the ILC operating at $\sqrt{s} = 500\,\text{GeV}$. *LC-REP-2013-007.*

[173] Wolfgang Kilian, Thorsten Ohl, and Jurgen Reuter. WHIZARD: Simulating Multi-Particle Processes at LHC and ILC. *Eur.Phys.J.*, C71:1742, 2011.

[174] Mauro Moretti, Thorsten Ohl, and Jurgen Reuter. O'Mega: An Optimizing matrix element generator. *IKDA-2001-06, LC-TOOL-2001-040, hep-ph/0102195*, 2001.

[175] Erik Devetak, Andrei Nomerotski, and Michael Peskin. Top quark anomalous couplings at the International Linear Collider. *Phys.Rev.*, D84:034029, 2011.